# Franck-Condon principle and the hadronic and muonic Auger effect

J. E. Russell
*Physics Department, University of Cincinnati, Cincinnati, Ohio 45221-0011*
(Received 14 October 1997; revised manscript received 23 February 1998)

Auger rates are calculated for some unrealistically low-lying states of antiprotonic helium. Two methods are used. One method, which makes use of hydrogenic functions and the golden rule, should give accurate rates. The other method treats the Auger process as inelastic scattering in one dimension. It makes use of a two-state approximation and the modern Born-Oppenheimer approximation, and it relates the transition rate to a ratio of probability currents for radial motion on two coupled one-dimensional adiabatic potential surfaces with an avoided crossing. In most instances this method leads to good agreement with the golden rule if only one traversal of the crossing is taken into account, and it demonstrates that the transition can be thought of as occurring at a rather well-defined radial separation between the $\bar{p}$ and the nucleus, in accord with the Franck-Condon principle. It is found that taking into account many traversals of the crossing would lead to fairly good agreement with the golden rule if the phases of the separate contributions to the transition amplitude from these traversals are effectively random. It is argued that radial and (perhaps) angular motion would ultimately produce the requisite phases if the finite width of the initial state were to be taken into account. The calculations for antiprotonic helium are then used as the basis for a conjecture that a phase difference associated with the angular motion of a stopping $\mu^-$, $\pi^-$, or $K^-$ might largely account for the very striking, shell-dependent regularities that have been observed in x-ray yields from exotic atoms formed in heavier elements.
[S1050-2947(98)02307-5]

PACS number(s): 36.10.−k

## I. INTRODUCTION

This paper is motivated in part by the belief that the Franck-Condon principle (FCP), which was first enunciated to account for variations in the intensity of molecular band spectra [1,2], must also govern Auger transitions in highly excited states of exotic atoms. In either instance there is a sudden, drastic rearrangement of an otherwise almost adiabatically varying electronic structure. The basic idea of FCP is that the drastic change in the motion of the rapidly moving electrons occurs so quickly that the much more slowly moving massive particles—whose motion is in most instances nearly classical (in the sense that their positions and momenta can be thought of as being simultaneously rather well defined)—experience very little impulse. As a result, a transition tends not to proceed unless the massive particles are momentarily situated so that their momenta are nearly the same in both the initial and final states.

The FCP is ordinarily thought of only with regard to radial motion; and most of the discussion in the present paper is with regard to radial motion. We shall, however, raise the question as to the possible relevance of angular separations between points on a two-dimensional classical trajectory where a transition can be thought of as occurring, especially a transition that occurs during exotic atom formation (EAF). Although most of the calculations in the present paper are quantum-mechanical and are for radial motion alone, we shall in some instances speak in terms of classical trajectories in two dimensions, and we shall assume that it would be meaningful to associate quantum-mechanical phases with such trajectories, as has been done for some chemical reactions [3], though usually in just one dimension. Specifically, we shall conjecture that a phase difference due to different angular momenta on segments of different, almost classical paths leading to the same final state might account for the very striking, shell-dependent regularities in x-ray yields from muonic, pionic, and kaonic atoms that became the focus of much attention many years ago after Wiegand and Godfrey conducted a systematic study of negative kaons stopping in pure elements [4–6].

It was found in Refs. [4–6] that the angular momentum $L$ of the captured particle is correlated with the position of the capturing atom in the Periodic Table, with a relatively high $L$ being more likely near closed shells. Later studies, mostly of muons stopping in chemical compounds, revealed another (apparently related) shell effect, this one involving the total capture cross section, which was found to be relatively small near closed shells [7–9]. We note that these effects are consistent with there being some mechanism(s) causing capture of particles with relatively low $L$ to be suppressed near closed shells. We further note that this would be consistent with there being some sort of $L$-dependent interference that also depends on shell structure.

EAF is not well understood theoretically, especially with regard to the distribution of energy and angular momentum of the newly captured hadron or muon. This has occasionally been noted in the literature [10,11]. The number of theoretical papers on EAF is vast, stretching back over half a century [12]. Even within the past few years there have been more investigations [13–15]. A variety of approaches have been employed, many of them making use, in one way or another, of the assumption that the stopping particle behaves in some respects like a classical particle. Also, it has long been recognized that the response of the electrons in the capturing atom to the stopping particle is in some respects almost adiabatic. However, the possibility that in some instances a decisive role might be played by interference between two different contributions to the transition amplitude—each

 

associated with a fairly well-defined position of the stopping particle, in accord with the FCP—seems not to have been considered in any previous study. The present paper seeks to establish that this possibility is entirely consistent with an elementary example of the hadronic Auger effect.

For simplicity, we restrict our attention to hypothetical instances for which the calculation of Auger rates becomes relatively easy, but our primary purpose is to uncover features of Auger transitions that might be important in EAF. We present no calculations for muonic, pionic, or kaonic atoms. Instead, we restrict our attention to antiprotonic helium ($\bar{p}\mathrm{He}^+$), which consists only of a helium nucleus, a $\bar{p}$ with large principal quantum number $N$, and an electron in its ground state. Moreover, even for this atom we make some simplifications. We assume the mass of the helium nucleus to be infinite, which frees us from having to include a Fried-Martin correction [16]. Although our calculations of $\bar{p}$ radial motion are in most instances quantum mechanical, we require $N$ to be large enough so that the (unperturbed) radial motion is almost classical, except for circular and nearly circular orbitals. We also require the energy difference between adjacent principal levels to be large enough to permit Auger ejection. Specifically, we consider only instances in which $N=10$ or 15. The $\bar{p}$ mean orbital radius is then at least 15 times smaller than that of the electron, which greatly simplifies the computation of wave functions. (These examples are indeed hypothetical because $\bar{p}\mathrm{He}^+$ with $N\leqslant 15$ does not exist: the $\bar{p}$ is initially captured into an atomic orbital with much higher $N$ and, sooner or later, is annihilated before it can reach $N=15$ [17].)

Accurate Auger rates for these simple hypothetical examples are easily computed with the golden rule, and we shall use these rates as a basis for comparison. In our golden rule calculations the wave functions for the unperturbed states are assumed to be hydrogenic, and the perturbing interaction is assumed to be the dipole electrostatic interaction between the electron and the $\bar{p}$. Though we present no systematic description of these calculations, which are similar to ones performed many years ago for muonic atoms by Burbidge and de Borde [18], we will note from time to time the similarity of some of their features to those of the calculations that are the subject of most of the present paper.

In this paper we devise another way of computing Auger rates in order to argue that a transition can usefully be thought of as occurring at a fairly well-defined radial separation between the $\bar{p}$ and the nucleus, in accord with the FCP. (A preliminary report of these calculations has already appeared [19].) Our estimates of Auger rates are made using probability currents for $\bar{p}$ motion on two coupled one-dimensional adiabatic potential surfaces with an avoided crossing. We are able to use probability currents because the motion on the adiabatic surfaces is almost classical in some instances. In effect, we treat an Auger transition between two almost stationary bound states as a Landau-Zener-Stückelberg (LZS) process, which is ordinarily thought of as a special type of inelastic scattering. We shall regard the probability current for the final state as being proportional to the absolute square of a time-dependent transition amplitude, with the time in each instance being the total time required for the $\bar{p}$, treated as a classical particle, to complete an integral number of half-cycles of motion in the initial state. Furthermore, the *angular* action that would be associated with the nearly classical motion on the adiabatic surfaces is used in some instances to estimate quantum-mechanical phases and phase differences that might be present if the time-dependent transition amplitude were to be expressed as a sum of terms, each associated with a different, more or less classical, path leading to the same final state [3,20,21].

Our probability currents are computed using Born-Oppenheimer (BO) wave functions, but within the framework of the modern BO approximation [22,23]. There are two reasons why we use BO functions. One reason is that their use is conceptually convenient: in principle, the final electron wave function can be related to the time-dependent transition amplitude, and the relative phases of the contributions to this wave function from separate encounters of the $\bar{p}$ with the avoided crossing can be specified approximately in terms of integrals of a diagonal element of the vector potential that characterizes the modern BO approximation. The second reason is to call attention to some of the difficulties, and also to some of the advantages, of using BO functions and the modern BO approximation to calculate Auger rates for the much more highly excited states of $\bar{p}\mathrm{He}^+$ that have actually been observed [17].

The electronic BO wave functions used in this paper are not exact. Though it is possible to determine the adiabatically varying electronic BO function for $\bar{p}\mathrm{He}^+$ precisely for the initial state [24,25], the calculation would be lengthy, and for this reason we use first-order perturbation theory. The final electron wave function is approximated with a Coulomb wave. Our electronic functions are believed to be accurate enough for the low-lying transitions considered here.

Our calculations are carried only to lowest nonvanishing order in the $\bar{p}$-nucleus separation. We use atomic units.

### Outline of paper

Section II is devoted to a calculation of wave functions. The initial and final states of the $\bar{p}$, together with the vector potential necessary to specify the nonadiabatic coupling between them, are discussed in Sec. II A. Our approximate electronic functions are presented in Sec. II B. These functions are then used in Sec. II C to estimate off-diagonal elements of the vector potential. Section II D is devoted to three equivalent sets of coupled differential equations, each describing the radial motion of the $\bar{p}$, but in different ways. The first of these, which is a set of equations obtained directly from the modern BO approximation, contains first derivatives in its coupling terms. The second set is obtained from the first by a unitary transformation that achieves a diabatic representation in which the coupling terms contain no first derivative, thereby ensuring that the sum of probability currents remains precisely constant. The third set is obtained from the second by another unitary transformation that results in equations for motion on adiabatic potential surfaces, where the radial motion is almost classical in some instances.

Section III is devoted to the calculation of Auger rates, in most instances with probability currents. As outlined in Sec. III A, our calculation of an Auger rate using currents begins

with a truncated set of starting values of a regular solution of the radial wave equation for $\bar{p}$ motion on the diabatic surfaces, obtained at a very small radial separation by using procedures described in Sec. II D. These starting values are chosen so that there is appreciable relative amplitude on only one of the two surfaces. It is combined with another suitably chosen, independent set of starting values to give a traveling wave initially moving outward, but only on the one surface. The wave is determined at larger separations by numerical integration of coupled differential equations. As outlined in Sec. III B, approximations of several successive reflections of this wave are found by further numerical integration. In Sec. III C, some arguments are presented to justify a preliminary expression for the Auger rate in terms of unreflected outgoing currents on the diabatic surfaces. This expression is then modified for use with unreflected currents on the adiabatic surfaces. A brief discussion of Auger rates in terms of time-dependent probabilities rather than probability currents is also included, partly to emphasize some of the shortcomings of our two-state model, and partly to note the seeming importance of the contributions to the actual time-dependent transition amplitude from separate half-cycles of (almost classical) $\bar{p}$ motion. Numerical estimates of Auger rates obtained with probability currents are presented in Sec. III D. These estimates are made using reflected as well as unreflected waves on the adiabatic surfaces, with further suitable modifications of the expression for the Auger rate. Our numerical results, together with some considerations prompted by work of chemists [3,20,21], lead us to conclude that the actual time-dependent transition amplitude can be thought of as a sum of many terms, all of them of nearly equal magnitude, and each of them due to a radially rather well-defined encounter of the $\bar{p}$ with an avoided crossing between two adiabatic potential surfaces, in accord with the FCP. It is concluded in Sec. III E that effectively random phase differences between the contributions from these encounters must exist if agreement with the golden rule is to be achieved, and it is argued that radial and (perhaps) angular motion of the $\bar{p}$ would produce the required differences if the finite width of the initial state were to be taken into account. *Also, it is conjectured that phase differences due to angular motion might be important in EAF, and that they could be estimated using classical mechanics.*

The discussion in Sec. IV is devoted to two items. One is the possibility of using the modern BO approximation in a golden rule calculation of Auger rates for the highly excited states of $\bar{p}\mathrm{He}^+$ that have actually been observed. The other is our conjecture that phase differences due to angular motion might account for the experimental results reported in Refs. [4–9].

One other matter is worth mentioning here. Many of our numerical results depend on a multiplicative factor denoted by $f_r$. As explained in more detail in Sec. II D 4, our computer program was unable in most instances to obtain solutions of the radial wave equations unless the perturbing interaction responsible for Auger transitions was multiplied by $f_r \ll 1.0$. In most instances we set $f_r = 0.01$. We believe this procedure did not lead to any significant inaccuracy, because in almost all of our calculations the transition amplitudes and the relevant differences in energy and phase were found to vary linearly with $f_r$. The only exception is a phase difference shown in Figs. 13 and 14. This exception is carefully discussed in Sec. III E 4.

## II. WAVE FUNCTIONS

We work within the framework of a two-state approximation, and we use some of the mathematical apparatus of the modern BO approximation. The initial and final electron wave functions are denoted by $\psi_1(\mathbf{R},\mathbf{r})$ and $\psi_2(\mathbf{R},\mathbf{r})$, where $\mathbf{r}$ is the position of the electron. Both functions are assumed to depend adiabatically on the position $\mathbf{R}$ of the $\bar{p}$, as in a traditional BO calculation. The initial electron is bound in a slightly distorted $1s$ state. The final electron is in the continuum with momentum $k$. In most applications of the BO approximation, electronic energies depend in a significant way on the spacing(s) between the massive particles, but we can write them here simply as

$$(\text{initial electron energy}) = \epsilon_1 = -\tfrac{1}{2},$$

$$(\text{final electron energy}) = \epsilon_2 = +\tfrac{1}{2}k^2.$$

This is correct by definition in the latter instance and correct to first order in $R$ in the former. The final electron wave function $\psi_2$ is, of course, degenerate with respect to a nondenumerably infinite number of other states. This will be taken into account later in estimating transition rates, but it is not taken into account in our BO calculations, as we are restricting ourselves to the consideration of just two coupled states. Some of the complexities associated with degeneracies in a modern BO calculation are ignored here [26].

The initial and final states of the $\bar{p}$ are denoted by $\Psi_1(\mathbf{R})$ and $\Psi_2(\mathbf{R})$. They are assumed to be nearly hydrogenic with

$$(\text{initial principal quantum number}) = N,$$

$$(\text{final principal quantum number}) = N - \Delta N,$$

$$(\text{initial angular momentum and } z \text{ component}) = L,$$

$$(\text{final angular momentum and } z \text{ component}) = L - 1.$$

If transitions are caused predominantly by the $E1$ interaction, as should be the case if the $\bar{p}$ is deep within the atom, the initial and final angular momenta can differ by only one unit. Golden rule calculations show that transitions with a decrease in $\bar{p}$ angular momentum are much more favored than those with an increase. (This can be understood in terms of the FCP [19].) The reason for assuming that the angular momentum and its $z$ component are equal to each other in both the initial and the final state is that the rate for a transition between these two states is equal to the rate obtained by taking into account all possible $z$ components of the initial and final angular momenta, with a sum over the latter and an average over the former.

### A. Antiproton wave functions

In all of our calculations the final electron energy $\epsilon_2$ is assumed to be such that the two BO states, $\Psi_1(\mathbf{R})\psi_1(\mathbf{R},\mathbf{r})$ and $\Psi_2(\mathbf{R})\psi_2(\mathbf{R},\mathbf{r})$, have equal energies, as computed in the

traditional way without taking into account any coupling between them. However, our computation of $\Psi_1$ and $\Psi_2$ does take into account coupling. We write the initial and final $\bar{p}$ wave functions in the form

$$\Psi(\mathbf{R})=\begin{pmatrix}\Psi_1(\mathbf{R})\\ \Psi_2(\mathbf{R})\end{pmatrix}=\frac{1}{R}\begin{pmatrix}u_1(R)Y_{L,L}(\hat{\mathbf{R}})\\ u_2(R)Y_{L-1,L-1}(\hat{\mathbf{R}})\end{pmatrix}. \tag{1}$$

Later in this paper, in Sec. III, radial wave functions obtained by a unitary transformation from the functions $u_1$ and $u_2$ appearing in Eq. (1) are used to estimate Auger rates. To compute $u_1$ and $u_2$, we employ the modern BO approximation, and we *attempt* to regard the two-component column matrix $\Psi$ as an eigenfunction of the effective Hamiltonian

$$H_{\rm eff}=\frac{1}{2M}[\mathbf{P}-\mathbf{A}(\mathbf{R})]\cdot[\mathbf{P}-\mathbf{A}(\mathbf{R})]+V(R), \tag{2}$$

where $M$ is the mass of the $\bar{p}$, and $\mathbf{P}$, $\mathbf{A}$, and $V$ are

$$\mathbf{P}=-i\boldsymbol{\nabla}\begin{pmatrix}1&0\\0&1\end{pmatrix},$$

$$\mathbf{A}(\mathbf{R})=\begin{pmatrix}0&\mathbf{A}_{12}(\mathbf{R})\\ \mathbf{A}_{21}(\mathbf{R})&\mathbf{A}_{22}(\mathbf{R})\end{pmatrix}, \tag{3}$$

$$V(R)=\begin{pmatrix}-\frac{2}{R}+\epsilon_1&0\\ 0&-\frac{2}{R}+\epsilon_2\end{pmatrix}.$$

The matrix $\mathbf{A}$ is the vector potential characteristic of the modern BO approximation [22,23]. Its elements are defined by

$$\mathbf{A}_{mn}=\mathbf{A}_{nm}^{*}=i\int d^3\mathbf{r}\ \psi_m^{*}(\mathbf{R},\mathbf{r})\boldsymbol{\nabla}_{\boldsymbol{R}}\psi_n(\mathbf{R},\mathbf{r}), \tag{4}$$

where $\boldsymbol{\nabla}_{\boldsymbol{R}}$ is the gradient with respect to $\mathbf{R}$. Its off-diagonal elements are responsible for coupling between the $\bar{p}$ states $\Psi_1$ and $\Psi_2$. As discussed later, in Sec. II D 1, there are other states coupled to $\Psi_1$ and $\Psi_2$, but we shall ignore them. The diagonal elements of $V$ are the sums of the potential energy of the $\bar{p}$ in the field of the doubly charged nucleus and the initial or final electron energy. $H_{\rm eff}$ can be obtained using standard methods if the final electron state is treated as a nondegenerate bound state. As usual, a small term involving other electronic states has been neglected. We note that $H_{\rm eff}$ is the Hamiltonian for a model that is not realistic. The actual initial state of $\bar{p}\mathrm{He}^{+}$ is not stationary. In our model it is one of just two components of what will prove to be an *approximate* eigenfunction of $H_{\rm eff}$. We shall use this approximate eigenfunction in Sec. III as a starting point to compute an outward-traveling wave, which is then used to estimate a transition rate.

The following equations are pertinent to the approximations that will be made in Sec. II D 1, and they will also be referred to in Sec. IV A. $H_{\rm eff}$ can be written in the form

$$H_{\rm eff}=H_0+H', \tag{5}$$

where

$$H_0=\frac{1}{2M}\mathbf{P}\cdot\mathbf{P}+V(R), \tag{6a}$$

$$H'=\frac{1}{2M}[-\mathbf{P}\cdot\mathbf{A}(\mathbf{R})-\mathbf{A}(\mathbf{R})\cdot\mathbf{P}+\mathbf{A}(\mathbf{R})\cdot\mathbf{A}(\mathbf{R})]. \tag{6b}$$

Except for the constant terms $\epsilon_1$ and $\epsilon_2$ in $V$, the elements of the diagonal matrix $H_0$ are energy operators for a particle of mass $M$ moving in the Coulomb potential $-2/R$. We shall obtain coupled differential equations describing motion that takes into account only (i) those eigenfunctions of the (1,1) element of $H_0$ that are proportional to $Y_{L,L}$, and (ii) those eigenfunctions of the (2,2) element that are proportional to $Y_{L-1,L-1}$, the coupling being due to the perturbation $H'$. Furthermore, as outlined in Sec. II D 4, we shall require the radial functions $u_1$ and $u_2$ appearing in regular wave functions of the form given in Eq. (1) to resemble hydrogenic functions with principal quantum numbers $N$ and $N-\Delta N$.

The diagonal element $\mathbf{A}_{11}$ vanishes because $\psi_1$ has constant phase [27]. Though the diagonal element $\mathbf{A}_{22}$ does not vanish, we shall assume in our calculations that

$$\mathbf{A}_{22}(\mathbf{R})=0. \tag{7}$$

This simplifies the calculations, and we believe it should not significantly affect our estimates of transition rates with unreflected waves. However, the calculation of rates using reflected or multiply reflected waves is an entirely different matter, and the possible relevance of (a suitably modified form of) $\mathbf{A}_{22}$ to interference effects is discussed later, in Sec. III E 3. To compute the radial functions $u_1$ and $u_2$ in the $\bar{p}$ wave function $\Psi$, it is first necessary to obtain an explicit expression for $\mathbf{A}_{21}$ using suitable approximations to $\psi_1$ and $\psi_2$.

### B. Electron wave functions

We approximate the initial adiabatic electron wave function as

$$\psi_1(\mathbf{R},\mathbf{r})=\psi_{1s}(\mathbf{r})+\psi_p(\mathbf{R},\mathbf{r}),$$

where

$$\psi_{1s}(\mathbf{r})=\mathcal{R}_{1s}(r)/\sqrt{4\pi},\quad \mathcal{R}_{1s}(r)=2e^{-r},$$

$$\psi_p(\mathbf{R},\mathbf{r})=\mathcal{R}_p(R,r)\sqrt{3/4\pi}\ P_1(\hat{\mathbf{R}}\cdot\hat{\mathbf{r}}).$$

The term $\psi_{1s}$ is, of course, the normalized ground-state eigenfunction of the Hamiltonian,

$$H_e^{(0)}=-\frac{1}{2}\nabla^2-\frac{1}{r},$$

for an electron bound to an infinitely massive, singly charged nucleus. We regard $H_e^{(0)}$ as taking into account not only the interaction of the electron with the doubly charged nucleus, but also (approximately) its $E0$ interaction with the $\bar{p}$, the

latter interaction being equated to $1/r$ even if $r<R$. ($H_e^{(0)}$ and $\psi_{1s}$ are also the unperturbed Hamiltonian and initial wave function in our golden rule calculations.) The distortion $\psi_p$ is assumed to be small and to vary linearly with $R$. Therefore, $\psi_1$ is normalized to first order in $R$. We estimate $\mathcal{R}_p$, the radial amplitude of $\psi_p$, with first-order perturbation theory. We take into account (approximately) only the $E1$ interaction between the electron and the $\overline{p}$, this interaction being equated to

$$(4\pi/3)(R/r^2)\sum_m Y_{1,m}^*(\hat{\mathbf{R}})Y_{1,m}(\hat{\mathbf{r}})$$

even if $r<R$. (This is also the perturbing interaction in our golden rule calculations.) It is convenient to write

$$\mathcal{R}_p(R,r)=\mathcal{R}_p^{(b)}(R,r)+\mathcal{R}_p^{(c)}(R,r),$$

where $\mathcal{R}_p^{(b)}$ is due to excited bound states of $H_e^{(0)}$ and $\mathcal{R}_p^{(c)}$ is due to the continuum. A straightforward calculation shows that

$$\mathcal{R}_p^{(c)}(R,r)=R\int_0^\infty dk\ \mathcal{B}(k)\frac{F_1(kr)}{kr}, \tag{8}$$

where

$$\mathcal{B}(k)=\frac{2k^2}{\sqrt{3}\ \pi(\epsilon_1-\epsilon_2)}\int_0^\infty dr\ \mathcal{R}_{1s}(r)\frac{F_1(kr)}{kr}. \tag{9}$$

$F_1(kr)$ is the regular Coulomb wave function for a $p$-wave electron with energy $\epsilon_2=\frac{1}{2}k^2$. Our approximate expression for $\psi_1$ should be rather accurate for most values of $\mathbf{r}$. However, it is not accurate if $r\lesssim R$ because we have not used the proper functional forms of the $E0$ and $E1$ interactions for $r<R$, and also because we have neglected $E2$ and higher multipole interactions.

We approximate the final electron wave function $\psi_2$ with a suitable modification of the only important term in the partial wave expansion of the function used in our golden rule (GR) calculations. That function was

$$\psi_{\mathrm{GR}}(\mathbf{k}\cdot\mathbf{r})=4\pi\sum_l i^l e^{i\sigma_l}\frac{F_l(kr)}{kr}\sum_m Y_{l,m}^*(\hat{\mathbf{k}})Y_{l,m}(\hat{\mathbf{r}}). \tag{10}$$

$\psi_{\mathrm{GR}}$ is a Coulomb distorted plane wave, and the $\sigma_l$ and $F_l$ are the usual Coulomb phase shifts and wave functions. $\psi_{\mathrm{GR}}$ is an eigenfunction of $H_e^{(0)}$ with eigenvalue $\epsilon_2=\frac{1}{2}k^2$. It has unit density, and it satisfies the normalization condition

$$\int d^3k'\int d^3r\ \psi_{\mathrm{GR}}^*(\mathbf{k}'\cdot\mathbf{r})\ \psi_{\mathrm{GR}}(\mathbf{k}\cdot\mathbf{r})=(2\pi)^3.$$

Because only $E1$ transitions are important, and also because we only had to consider transitions between states in which the angular motion is described by $Y_{L,L}$ or $Y_{L-1,L-1}$, the only term in Eq. (10) that gave an appreciable contribution to our golden rule rates is

$$4\pi i e^{i\sigma_1}\frac{F_1(kr)}{kr}Y_{1,1}^*(\hat{\mathbf{k}})Y_{1,1}(\hat{\mathbf{r}}).$$

There is a one-to-one correspondence between this term and $\psi_{\mathrm{GR}}$, which means that the density of states, as a function of $\mathbf{k}$, is the same for both. For these reasons we find it convenient to approximate $\psi_2$ as

$$\psi_2(\mathbf{k},\mathbf{r})=\sqrt{4\pi}\frac{F_1(kr)}{kr}Y_{1,1}(\hat{\mathbf{r}}). \tag{11}$$

As indicated explicitly in Eq. (11), we regard $\psi_2$ as being $\mathbf{k}$ dependent, but with a value that depends only on the magnitude of $\mathbf{k}$, not its direction. Like $\psi_{\mathrm{GR}}$, it satisfies the normalization condition

$$\int d^3k'\int d^3r\ \psi_2^*(\mathbf{k}',\mathbf{r})\psi_2(\mathbf{k},\mathbf{r})=(2\pi)^3.$$

As with $\psi_1$, our choice of $\psi_2$ is not accurate if $r\lesssim R$. Furthermore, it does not take into account a small distortion at $r\gg R$ associated with the momentary position $\mathbf{R}$ of the $\overline{p}$. This adiabatic distortion, which would be represented by small added terms due to the same $E1$ interaction that was taken into account in our approximation to $\psi_1$, would be proportional to $R$ and consequently should be unimportant if the calculation of $\mathbf{A}_{21}$ is carried only to first order in $R$, since $\boldsymbol{\nabla}_{\boldsymbol{R}}\psi_{1s}$ vanishes.

### C. Off-diagonal elements of vector potential

The calculation of $\mathbf{A}_{21}$ proceeds by standard methods. Determining the components of $\boldsymbol{\nabla}_{\boldsymbol{R}}\psi_1$ is straightforward. The integration over electron coordinates that must then be performed is easily accomplished using orthogonality relations. The orthogonality of energy eigenfunctions with different eigenvalues causes $\mathbf{A}_{21}$ to be independent of bound-state contributions to $\mathcal{R}_p$, and the relation

$$\int_0^\infty dr\ F_l(kr)F_l(k'r)=\frac{\pi}{2}\delta(k-k')$$

permits the integral over $k$ in Eq. (8) to be evaluated after the integration over $\mathbf{r}$ in Eq. (4) has been performed. The spherical components of $\mathbf{A}_{21}$ are

$$A_{21;R}=\mathcal{C}(k)\sin\Theta\ e^{-i\Phi}, \tag{12a}$$

$$A_{21;\Theta}=\mathcal{C}(k)\cos\Theta\ e^{-i\Phi}, \tag{12b}$$

$$A_{21;\Phi}=-i\mathcal{C}(k)e^{-i\Phi}, \tag{12c}$$

where

$$\mathcal{C}(k)=-i(\pi/k)^2\mathcal{B}(k)/\sqrt{2\pi},$$

and $\Theta$ and $\Phi$ are the angular coordinates of the $\overline{p}$. The validity of these simple expressions, which are independent of $R$ since $\mathcal{R}_p\propto R$, depends on the mean orbital radius of the $\overline{p}$ being much smaller than that of the electron.

### D. Antiproton radial wave equations

#### 1. Equation obtained from modern BO approximation

We now introduce further approximations and obtain a set of relatively simple differential equations for the functions $u_1$ and $u_2$ appearing in Eq. (1). For the time being, we neglect the term in $H_{\rm eff}$ containing $\mathbf{A}\cdot\mathbf{A}$, as it should lead only to second-order effects. We *attempt* to write

$$H_{\rm eff}\Psi = E\Psi. \tag{13}$$

All derivatives with respect to the $\bar{p}$ angular coordinates $\Theta$ and $\Phi$ on the left-hand side of this equation can be evaluated analytically. It is obvious from Eqs. (1)–(3), (7), and (12) that each term in a given component of the resulting expression has the same dependence on $\Phi$. This is not true of the dependence on $\Theta$. The vector potential $\mathbf{A}$, as we have written it in Eq. (12), couples the states $\Psi_1$ and $\Psi_2$, as we have written them in Eq. (1), not only to each other but also to states with angular momenta different from $L$ and $L-1$. We remedy this difficulty by simply neglecting the coupling with these other states. For the purpose of estimating Auger rates, this should be an acceptable procedure because we are only considering transitions whose rates can be calculated reliably using first-order perturbation theory. We eliminate coupling to these other states by multiplying both sides of Eq. (13) by

$$\begin{pmatrix} Y^*_{L,L}(\hat{\mathbf{R}}) & 0 \\ 0 & Y^*_{L-1,L-1}(\hat{\mathbf{R}}) \end{pmatrix}$$

and integrating over $\hat{\mathbf{R}}$. We note that if we had retained the term in $H_{\rm eff}$ proportional to $\mathbf{A}\cdot\mathbf{A}$, this integration would have caused its contribution to vanish. The resulting equation for $u_1$ and $u_2$ can be written as the eigenvalue equation

$$-\frac{1}{2M}\frac{d^2u}{dR^2} + \mathcal{U}u = Eu, \tag{14}$$

where

$$u = \begin{pmatrix} u_1(R) \\ u_2(R) \end{pmatrix}, \quad \mathcal{U} = \begin{pmatrix} \mathcal{U}_{11}(R) & \mathcal{U}_{12}(R) \\ \mathcal{U}_{21}(R) & \mathcal{U}_{22}(R) \end{pmatrix}.$$

The elements of $\mathcal{U}$ are given by

$$\mathcal{U}_{11}(R) = \frac{L(L+1)}{2MR^2} - \frac{2}{R} + \epsilon_1,$$

$$\mathcal{U}_{12}(R) = \frac{1}{M}\,\mathcal{D}_L(k)\left(\frac{L}{R} - \frac{d}{dR}\right),$$

$$\mathcal{U}_{21}(R) = \frac{1}{M}\mathcal{D}_L(k)\left(\frac{L}{R} + \frac{d}{dR}\right),$$

$$\mathcal{U}_{22}(R) = \frac{(L-1)L}{2MR^2} - \frac{2}{R} + \epsilon_2,$$

where

$$\mathcal{D}_L(k) = \pi^{3/2}\sqrt{\frac{L}{2L+1}}\,\frac{\mathcal{B}(k)}{k^2}. \tag{15}$$

The precise value of $E$ for a regular solution of Eq. (14) depends on $N$, $L$, $\Delta N$, and the assumed value of $k$. It also depends on the assumed relative sign of $u_1$ and $u_2$ at very small $R$.

We shall refer to the diagonal elements $\mathcal{U}_{11}$ and $\mathcal{U}_{22}$ as the unperturbed initial and final effective radial potentials. It is argued in Sec. III that an Auger transition can be thought of as occurring in the vicinity of the point where these two potentials become equal to one another. The perturbation responsible for Auger transitions is proportional to $\mathcal{D}_L(k)$, which appears in the off-diagonal elements of $\mathcal{U}$. We note that even though Eq. (14) is for the radial wave functions alone, the perturbation coupling $u_1$ and $u_2$ depends on angular motion. The term in $\mathcal{U}_{21}$ containing the derivative with respect to $R$ obviously is associated only with the radial component of $\mathbf{A}_{21}$. But the other term, the one proportional to $L/R$, is a sum of contributions associated with the angular components as well as the radial component. A detailed examination of these contributions reveals that the one associated with the component $A_{21;\Theta}$ is relatively quite small unless $L$ is quite small. But the contribution associated with azimuthal motion is relatively large if $L$ is relatively large. *This provides part of the basis for a conjecture, outlined in Secs. III E 3 and IV B, that phase differences due to angular motion might be important in EAF and that they could be estimated using classical mechanics.*

Our method of estimating Auger rates, as outlined in Sec. III, depends on the radial motion of the $\bar{p}$ being nearly classical for certain values of $R$. If this condition is to be fulfilled, it is necessary not only that the $\bar{p}$ local wavelengths not be changing too rapidly, but also that the coupling between the electronic states depend adiabatically on the position of the $\bar{p}$. An approximate description of adiabatic motion can be achieved by a unitary transformation. The motion is indeed adiabatic if it is permissible to ignore the off-diagonal elements in the transformed equation. This is not always possible; but it is possible to cause the off-diagonal elements in a transformed equation to be truly important only for a comparatively narrow range of $R$. Because of the presence of a derivative in the off-diagonal elements of $\mathcal{U}$, we accomplish this by two successive transformations, both expressed in a familiar general form [22,28].

#### 2. Equation for diabatic representation

The purpose of the first transformation is to obtain an expression similar to Eq. (14), but containing no first derivative. We accomplish this by writing

$$u = U_a v, \tag{16}$$

where

$$U_a = \begin{pmatrix} \cos\Omega_a & -\sin\Omega_a \\ \sin\Omega_a & \cos\Omega_a \end{pmatrix}, \quad v = \begin{pmatrix} v_1(R) \\ v_2(R) \end{pmatrix} \tag{17}$$

and

$$\Omega_a = \mathcal{D}_L(k)R.$$

The equation for $v$ then becomes

$$-\frac{1}{2M}\frac{d^2v}{dR^2} + \mathcal{V}v = Ev, \tag{18}$$

where the elements of

$$\mathcal{V} = \begin{pmatrix} \mathcal{V}_{11}(R) & \mathcal{V}_{12}(R) \\ \mathcal{V}_{21}(R) & \mathcal{V}_{22}(R) \end{pmatrix}$$

are given by

$$\mathcal{V}_{11} = -\frac{2}{R} + \left(\frac{L(L+1)}{2MR^2} + \epsilon_1\right)\cos^2\Omega_a - \frac{1}{2M}[\mathcal{D}_L(k)]^2 + \left(\frac{(L-1)L}{2MR^2} + \epsilon_2\right)\sin^2\Omega_a + \frac{1}{M}\mathcal{D}_L(k)\frac{L}{R}\sin 2\Omega_a,$$

$$\mathcal{V}_{12} = -\frac{1}{2}\left(\frac{L(L+1)-(L-1)L}{2MR^2} + \epsilon_1 - \epsilon_2\right)\sin 2\Omega_a + \frac{1}{M}\mathcal{D}_L(k)\frac{L}{R}\cos 2\Omega_a,$$

$$\mathcal{V}_{21} = \mathcal{V}_{12},$$

$$\mathcal{V}_{22} = -\frac{2}{R} + \left(\frac{(L-1)L}{2MR^2} + \epsilon_2\right)\cos^2\Omega_a - \frac{1}{2M}[\mathcal{D}_L(k)]^2 + \left(\frac{L(L+1)}{2MR^2} + \epsilon_1\right)\sin^2\Omega_a - \frac{1}{M}\mathcal{D}_L(k)\frac{L}{R}\sin 2\Omega_a.$$

Though more complicated in form, the diagonal elements $\mathcal{V}_{11}$ and $\mathcal{V}_{22}$ are not very different from the unperturbed effective radial potentials $\mathcal{U}_{11}$ and $\mathcal{U}_{22}$. Since $\mathcal{V}_{12} = \mathcal{V}_{21}$, the Wronskian—or, equivalently, the total probability current—for Eq. (18) is constant. The off-diagonal elements of $\mathcal{V}$ can be thought of as causing transitions from one of the diabatic potential surfaces, $\mathcal{V}_{11}$ or $\mathcal{V}_{22}$, to the other. $\mathcal{V}_{12}$ is shown in Fig. 1 for $L=2$ and 14, in both instances for $N=15$ and $\Delta N=-1$. The range of $R$ in this figure includes all separations relevant to our calculations. $\mathcal{V}_{12}$ is very nearly proportional to $\Omega_a = \mathcal{D}_L(k)R$, which makes it difficult to think of a transition between $\mathcal{V}_{11}$ and $\mathcal{V}_{22}$ as occurring at a well-defined separation. Partly for this reason, but mostly because $\mathcal{V}_{12}$ is generally not small enough to permit motion on the diabatic surfaces to be regarded as almost classical, we shall consider adiabatic potential surfaces, where the motion of the $\overline{p}$ is in some instances much more nearly classical. We note that the angle $\Omega_a$ specifying the transformation between the radial wave functions $u$ and $v$, which is given approximately by

$$\Omega_a \approx \frac{\mathcal{V}_{12}}{\epsilon_2 - \epsilon_1}, \tag{19}$$

where

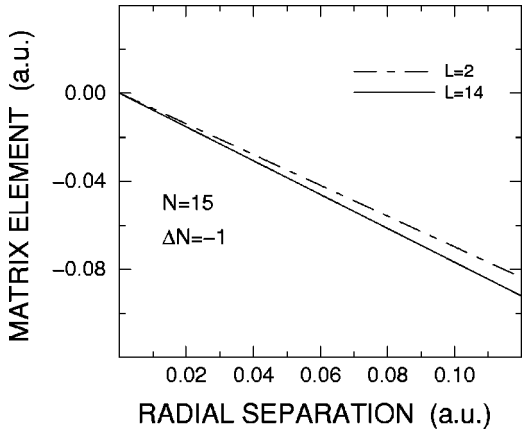


FIG. 1. The matrix element $\mathcal{V}_{12}$ for $L=2$ and 14, in both instances for $N=15$ and $\Delta N=-1$.

$$(\epsilon_2 - \epsilon_1) = 2.41 \text{ a.u. if } N=15 \tag{20}$$

is small enough in every instance so that the angular motion associated with the upper (lower) component of $v$ should not be very different from that associated with the upper (lower) component of $u$.

### *3. Equation for adiabatic representation*

A description of nearly adiabatic motion is achieved by a second transformation, which we write as

$$v = U_b w, \tag{21}$$

where

$$U_b = U_b^{-1} = \begin{pmatrix} \cos\Omega_b & \sin\Omega_b \\ \sin\Omega_b & -\cos\Omega_b \end{pmatrix}, \quad w = \begin{pmatrix} w_1(R) \\ w_2(R) \end{pmatrix}.$$

It is straightforward to show that

$$U_b^{-1}\mathcal{V}U_b = \mathcal{W} = \begin{pmatrix} \mathcal{W}_+(R) & 0 \\ 0 & \mathcal{W}_-(R) \end{pmatrix},$$

where

$$\mathcal{W}_\pm = \tfrac{1}{2}(\mathcal{V}_{11} + \mathcal{V}_{22}) \pm \tfrac{1}{2}\sqrt{(\mathcal{V}_{11} - \mathcal{V}_{22})^2 + (2\mathcal{V}_{12})^2},$$

if

$$\sin 2\Omega_b = \frac{2\mathcal{V}_{12}}{\sqrt{(\mathcal{V}_{11} - \mathcal{V}_{22})^2 + (2\mathcal{V}_{12})^2}}, \tag{22a}$$

$$\cos 2\Omega_b = \frac{\mathcal{V}_{11} - \mathcal{V}_{22}}{\sqrt{(\mathcal{V}_{11} - \mathcal{V}_{22})^2 + (2\mathcal{V}_{12})^2}}. \tag{22b}$$

$\mathcal{W}_+(R)$ and $\mathcal{W}_-(R)$ are, of course, the usual expressions for adiabatic potentials with an avoided crossing that appear in many discussions of LZS transitions. The equation for $w$ is

$$-\frac{1}{2M}\frac{d^2w}{dR^2}+\left[\mathcal{W}+\frac{1}{2M}\left(\frac{d\Omega_b}{dR}\right)^2\right]w$$
$$+\frac{1}{2M}\begin{pmatrix}0 & -1\\ 1 & 0\end{pmatrix}\left(2\frac{d\Omega_b}{dR}\frac{dw}{dR}+\frac{d^2\Omega_b}{dR^2}w\right)=Ew. \qquad (23)$$

Figure 2 shows the upper and lower adiabatic potentials $\mathcal{W}_+$ and $\mathcal{W}_-$ for several values of $L$, in each instance for $N=15$ and $\Delta N=-1$. A different energy scale is used for each $L$. The total energy of the system is also shown, but only for separations classically allowed for both potentials. In each instance the avoided crossing is located well within the classically allowed region, in accord with the FCP. To the level of accuracy visible in Fig. 2, $\mathcal{W}_+$ and $\mathcal{W}_-$ are indistinguishable from the diagonal elements of $\mathcal{U}$ or $\mathcal{V}$, provided the solid and the dashed curves to the right of the avoided crossings are thought of as being interchanged.

Equation (23), like Eqs. (14) and (18), has off-diagonal elements that cannot in general be ignored. However, the off-diagonal elements in Eq. (23) depend on derivatives of $\Omega_b$, and these derivatives are large only for a relatively small range of $R$. As illustrated in Figs. 3 and 4, the off-diagonal elements in Eq. (23) are truly important only within a narrow range, which makes it possible to think of a transition (or the lack of one) from one adiabatic surface to the other as occurring at a fairly well-defined separation.

Figure 3(a) shows $\Omega_b$ for all separations classically allowed on both $\mathcal{W}_+$ and $\mathcal{W}_-$. This angle, which is nearly zero for most separations below the avoided crossing, suddenly approaches $-\pi/2$ as $R$ passes the crossing; but then, for all but the largest $L$, $\Omega_b$ slowly rises a bit. As discussed in Sec. III D, this slow rise proves to be troublesome in estimating Auger rates. A detailed view of the increase in $\Omega_b$ at large $R$ is given in Fig. 3(b), which also shows its minimum. The slight rise in $\Omega_b$ at large separations notwithstanding, the overall behavior of this angle, as shown in Fig. 3(a), together with the very small values of $\Omega_a$ estimated in Sec. II D 2, indicate that, at all separations not too near the crossing, the angular motion associated with a component of $w$ should not be very different from that associated with one or the other of the components of $u$. *This provides part of the basis for a conjecture, outlined in Secs. III E 3 and IV B, that phase differences due to angular motion might be important in EAF.*

Figure 4 shows three functions that resemble, more or less, functions which appear—or can be thought of as appearing—in Eq. (23), and which not only depend on a derivative of $\Omega_b$ but also multiply a component of $w$. The functions shown in Fig. 4 are defined by

$$T_1=\frac{1}{2M}\left(\frac{d\Omega_b}{dR}\right)^2,\quad T_2=\frac{k_c}{M}\left|\frac{d\Omega_b}{dR}\right|,\quad T_3=\frac{1}{2M}\left|\frac{d^2\Omega_b}{dR^2}\right|,$$

where $k_c$ is the local wave number for $v_1$ and $v_2$ at the point where the diabatic potentials $\mathcal{V}_{11}$ and $\mathcal{V}_{22}$ cross. $T_1$, $T_2$, and $T_3$ are all very sharply peaked near the crossing. $T_1$ is not associated with transitions. It is a diagonal term that must be added to both adiabatic potentials. It can be thought of as being responsible for a very small contribution to the energy $E$. We shall refer to $\mathcal{W}_\pm+T_1$ as a corrected adiabatic potential. $T_1$ causes these corrected potentials to be greater than $E$ at points very near the crossing. $T_2$ is a rough estimate of the magnitude of $\mathcal{T}_2$, which we define as

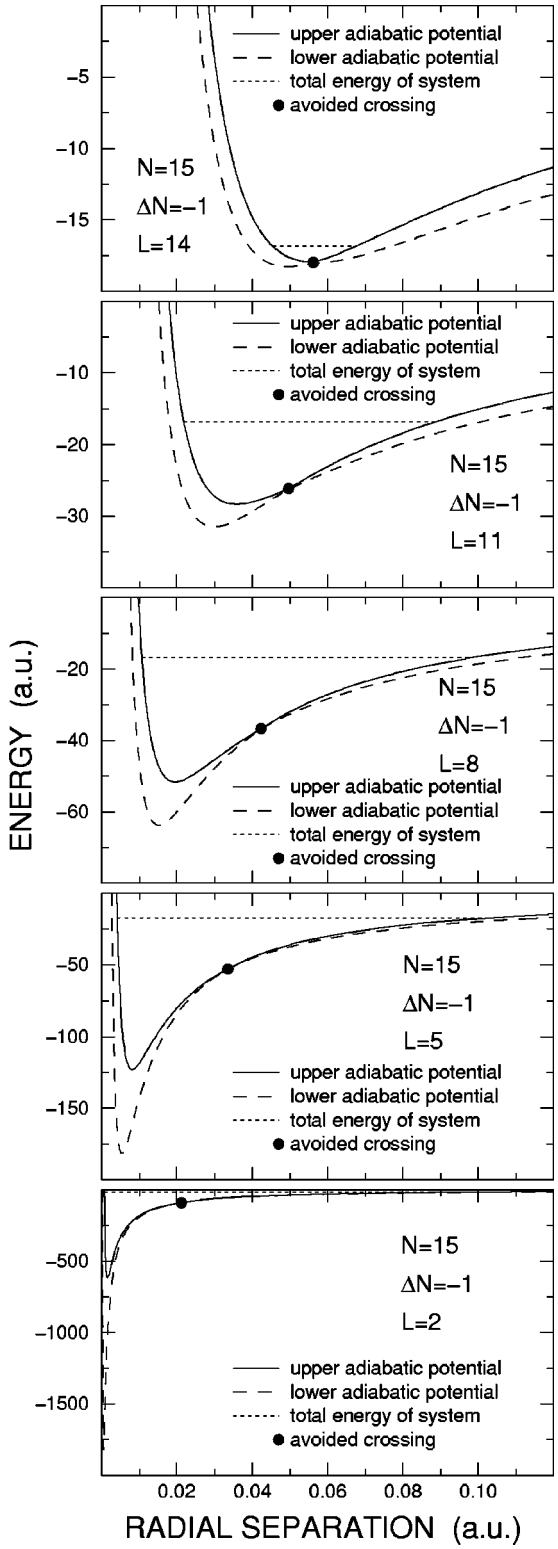


FIG. 2. Upper and lower adiabatic potentials $\mathcal{W}_+$ and $\mathcal{W}_-$ for several values of $L$, in each instance for $N=15$ and $\Delta N=-1$. The avoided crossing is marked. The total energy of the system is shown, but only for separations classically allowed for both potentials. A different energy scale is used for each $L$.

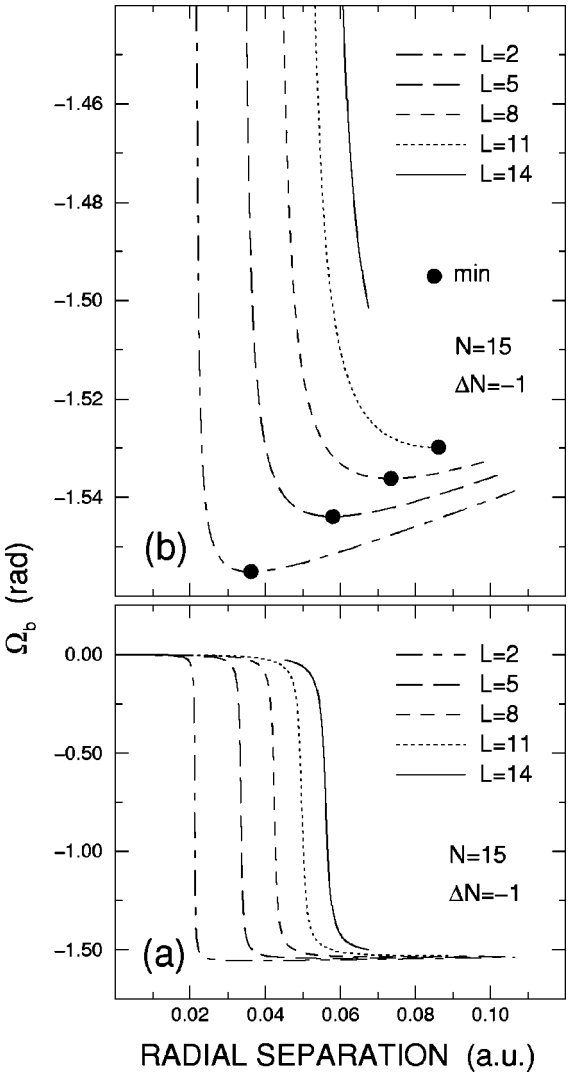


FIG. 3. The angle $\Omega_b$ for several values of $L$, in each instance for $N=15$ and $\Delta N=-1$. (a) For all separations classically allowed on both $\mathcal{W}_+$ and $\mathcal{W}_-$. (b) For a small range of $\Omega_b$, attainable only beyond the avoided crossing. $\Omega_b$ is shown on a greatly expanded scale, and its minimum is marked.

$$\mathcal{T}_2=\frac{1}{M}\frac{d\Omega_b}{dR}\frac{dw_1}{dR}\frac{1}{w_1}. \tag{24}$$

This function, which contains the reciprocal of $w_1$, can be thought of as appearing in Eq. (23) and multiplying $w_1$. There would, of course, be a similarly defined function with the opposite sign multiplying $w_2$. The terms in Eq. (23) containing first derivatives of both $\Omega_b$ and a component of $w$ are the terms generally believed to be of paramount importance in LZS transitions. Because of our introduction of the wave number $k_c$, the function $T_2$ can have quantitative significance only near the avoided crossing, and even there only for a solution of Eq. (23) representing a traveling wave; but this is not very restrictive, since our estimates of Auger rates in Sec. III are obtained with traveling waves, and our results are due largely to changes in currents occurring in the vicinity of crossings. $T_2$ vanishes at the point where $\Omega_b$ has a minimum and then increases somewhat as $R$ becomes larger. Because of the near absence of coupling, motion on the adiabatic

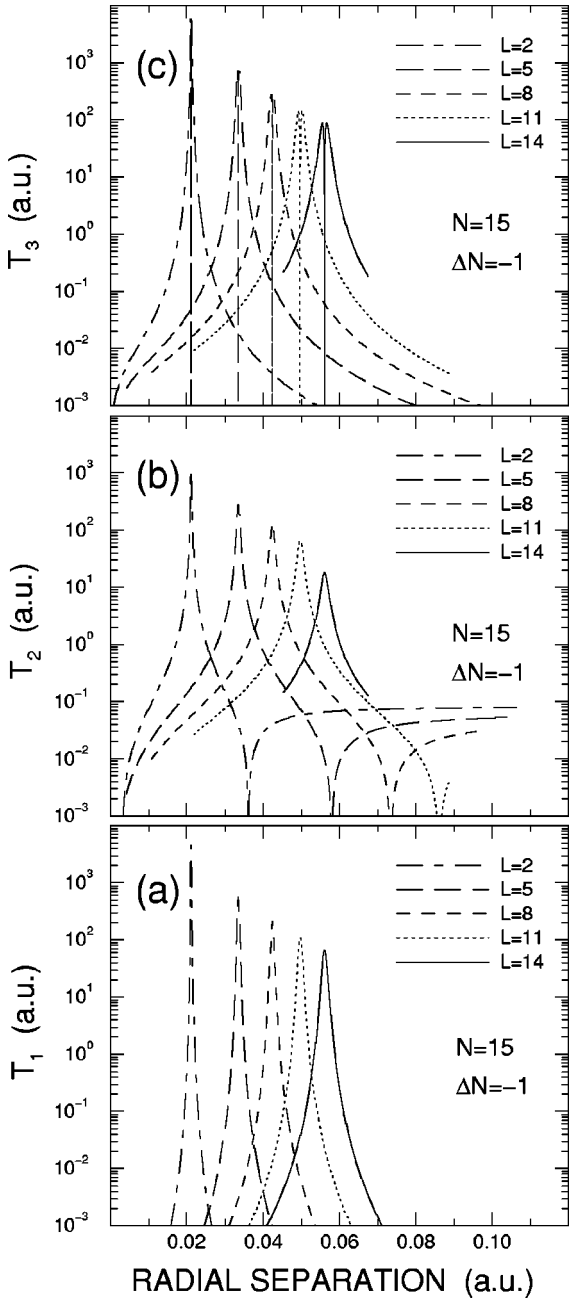


FIG. 4. The functions $T_1$, $T_2$, and $T_3$ for several values of $L$, in each instance for $N=15$ and $\Delta N=-1$. $T_2$ and $T_3$ are shown only for radial separations classically allowed on both $\mathcal{W}_+$ and $\mathcal{W}_-$.

surfaces should momentarily be almost classical at the point where $\Omega_b$ has a minimum, provided the local wavelengths on both surfaces are not changing too rapidly. However, even though $T_2$ has no quantitative significance at large separations, it seems clear that a certain amount of coupling between $w_1$ and $w_2$ reappears at large $R$ in some instances. This point is discussed again in Sec. III D. $T_3$ is the absolute value of $\mathcal{T}_3$, which we define as

$$\mathcal{T}_3=\frac{1}{2M}\frac{d^2\Omega_b}{dR^2}. \tag{25}$$

The function $\mathcal{T}_3$ appears in Eq. (23) and multiplies $w$. It varies rapidly near the avoided crossing, where it changes sign.

#### *4. Numerical procedures*

A knowledge of any one of the solutions $u$, $v$, or $w$ of Eqs. (14), (18), or (23) suffices to specify the other two. As will be explained in Sec. III B, a *regular* solution of Eq. (18) was used in obtaining approximate expressions for the reflections of traveling waves on the diabatic surfaces; as will be explained in Secs. III C and III D, these reflected waves were used to obtain similarly directed waves on the adiabatic surfaces, which were then used to estimate Auger rates. For these reasons we describe in some detail the procedures used to obtain accurate regular solutions of Eqs. (14), (18), and (23).

We used Gear's method, as implemented by the IMSL (International Mathematics and Statistics Library) subroutine DIVPAG, to obtain numerical solutions of one or another of the differential equations. It was decided not to integrate Eq. (14) anywhere because at very small $R$ its coupling terms diverge, while at very large $R$ they are not obviously less difficult to deal with than those of Eqs. (18) or (23). It was decided to integrate Eq. (18) rather than Eq. (23) in the classically allowed region, since the coupling terms in the latter vary so rapidly near the avoided crossing, but to integrate Eq. (23) at low separations because its coupling terms then become marginally smaller. Equation (23) was again selected at the very large separations for which classical motion is forbidden, in this instance because the potentials specified by the *diagonal* elements of $\mathcal{W}$, to a much greater extent than those of $\mathcal{V}$, are not too different from those of $\mathcal{U}$. At extremely large separations, a suitable solution of the equation for $u$, with the coupling terms $\mathcal{U}_{12}$ and $\mathcal{U}_{21}$ equated to zero, was calculated with standard methods, and then used to provide approximate starting values for an inward integration of the equation for $w$. A somewhat similar procedure was used at a very small separation to provide starting values for an outward integration.

Though we have, in effect, used uncoupled hydrogenic functions to estimate starting values for regular solutions of Eq. (23) at extremely small and very large $R$, the subsequent outward and inward numerical integrations to the region of classically allowed motion did take into account the coupling between $w_1$ and $w_2$. In the case of the inward integration, the two pairs of (uncoupled) starting values on the upper and lower adiabatic surfaces were each multiplied by suitably adjusted factors so as to obtain a solution that joined continuously near the higher classical turning points with the one obtained by the outward integration. A solution that varied smoothly everywhere was then achieved by adjusting the energy $E$ and the relative values of $w_1$ and $w_2$ and their derivatives at extremely small $R$.

We were not always able make the preceding scheme work without a modification. In many instances our computer program could not integrate Eq. (23) inward unless the quantity $\mathcal{D}_L$ defined in Eq. (15) was multiplied by a factor $f_r \ll 1$. We usually set $f_r = 0.01$. This improvisation ultimately led to satisfactory results because it was found in every instance that the probability current assumed to be proportional to the Auger rate varies almost precisely as $f_r^2$. All of the Auger rates reported in this paper that were estimated using probability currents were computed by setting $f_r = 0.01$ and then dividing the result by $f_r^2$.

For given values of $N$, $L$, $\Delta N$, and $k$, there are two regular solutions, which are linearly independent and which have slightly different energy eigenvalues. The ratio $v_2/v_1$—or, equivalently, $u_1/u_2$ or $w_1/w_2$—is positive at very small $R$ for one solution and negative for the other. The eigenvalues for these solutions are denoted by $E^+$ and $E^-$. (Our two-state model bears a passing resemblance to an asymmetric double well, the principal difference being that tunneling from one well to the other occurs at the crossing point, not at a classical turning point.) It was found that $E^+ - E^-$ is very nearly proportional to $f_r$.

For given values of $N$, $L$, $\Delta N$, and $k$, and for a given relative sign of $w_1$ and $w_2$ at very small $R$, the determination of the correct value of $E$ and the correct relative values of $w_1$ and $w_2$ and their derivatives is equivalent to a determination of the vibrational quantum number $n_v$ for the final state with the integral value

$$n_v = N - \Delta N - L. \tag{26}$$

This matter is discussed again in Sec. III C 1, where $n_v$ plays a role in our estimates of Auger rates.

Within the framework of our model, $k$ is a constant. We have already stated in Sec. II A that $\epsilon_2 = \frac{1}{2}k^2$ is assumed to be such that the energies of the BO states $\Psi_1\psi_1$ and $\Psi_2\psi_2$ are the same, provided all coupling between them is ignored. In practice we assume that $k$ is adequately specified by

$$\frac{1}{2}k^2 = -\frac{2M}{N^2} + \frac{2M}{(N-\Delta N)^2} - \frac{1}{2}, \tag{27}$$

since the initial and final states of both the electron and the $\bar{p}$ are nearly hydrogenic. Numerical calculations were always done using this expression. This matter is discussed again.

## III. ESTIMATES OF AUGER RATES

Most of our estimates of Auger rates are proportional to ratios of suitably specified probability currents for radial motion of the $\bar{p}$ on the one-dimensional adiabatic potential surfaces $\mathcal{W}_\pm$ appearing in Eq. (23). In essence, what is done is first to construct, at a suitably chosen small radial separation, a solution to this equation with a large outward current on $\mathcal{W}_+$ and a negligible current on $\mathcal{W}_-$. An outward numerical integration to a suitably chosen large separation is then performed, and the change in the currents is used to estimate the transition probability. Further calculations take into account some subsequent reflections. However, before presenting details of this seemingly *ad hoc* procedure, it is convenient to discuss probability currents for a simpler case, motion on the diabatic potential surfaces $\mathcal{V}_{11}$ and $\mathcal{V}_{22}$ appearing in Eq. (18).

Obtaining expressions for probability currents associated with solutions to Eq. (18) is trivial. The procedure is essentially the same as for single-component wave functions, and the results are essentially the same. The currents on $\mathcal{V}_{11}$ and $\mathcal{V}_{22}$ are

$$j_{v_1} = -\frac{i}{2M}\left( v_1^* \frac{dv_1}{dR} - \frac{dv_1^*}{dR} v_1 \right),$$

$$j_{v_2} = -\frac{i}{2M}\left( v_2^* \frac{dv_2}{dR} - \frac{dv_2^*}{dR} v_2 \right).$$

Their sum is

$$j_v = j_{v_1} + j_{v_2} = -\frac{i}{2M}\left( v^\dagger \frac{dv}{dR} - \frac{dv^\dagger}{dR} v \right). \tag{28}$$

This sum is constant for all values of $R$ because it is proportional to a Wronskian of a second-order differential equation containing no first derivative.

Probability currents can be meaningfully compared to experiment only if the motion is nearly classical. Because of this, we compute currents only in the region of positive kinetic energy, which we define for the time being to be the range of separations $R_{\rm lo} < R < R_{\rm hi}$ for which both of the potential energies $\mathcal{V}_{11}$ and $\mathcal{V}_{22}$ are less than $E$.

### A. Unreflected wave on diabatic surfaces

To compute the desired currents, we first specify a suitable wave function at $R_{\rm lo}$. We want to construct a function that can be thought of—if only in an approximate way—as describing purely outward motion. At separations near $R_{\rm lo}$ this motion should be almost exclusively on the surface $\mathcal{V}_{11}$. We begin by picking an *extremely small* separation $R_0 \ll R_{\rm lo}$, and we select the regular solution of Eq. (18) at $R = R_0$ with energy $E = E^+$, as defined in Sec. II D 4. (Choosing the regular solution with $E = E^-$ results in an estimated Auger rate almost the same as obtained with $E^+$.) However, we retain only $v_1$ and its derivative. We equate $v_2$ and its derivative to zero at $R_0$. This truncated solution provides starting values of a solution that will be denoted by $v^a$. We then integrate Eq. (18) outward to $R_{\rm lo}$. At this point $v_2^a$ has acquired a finite value, but it is still quite small compared to what it would have been otherwise. For the time being we define the real part of our complex wave function $v$ to be $v^a$. This definition will be slightly modified later. We represent the components of $v^a$ and their derivatives by a four-component vector function $\eta(R)$ defined by

$$\eta_1 = v_1^a, \quad \eta_2 = \frac{dv_1^a}{dR}, \quad \eta_3 = v_2^a, \quad \eta_4 = \frac{dv_2^a}{dR}. \tag{29}$$

We now determine an independent solution $v^b$ to Eq. (18). For the time being we define it to be the imaginary part of our complex wave function. This definition will be drastically modified later. We represent the components of $v^b$ and their derivatives by a four-component vector function $\xi(R)$ defined by

$$\xi_1 = v_1^b, \quad \xi_2 = \frac{dv_1^b}{dR}, \quad \xi_3 = v_2^b, \quad \xi_4 = \frac{dv_2^b}{dR}. \tag{30}$$

We choose to require $\xi$ to be orthogonal to $\eta$ at $R_{\rm lo}$. We satisfy this condition by writing $\xi(R_{\rm lo})$ in the form

$$\xi_1(R_{\rm lo}) = \alpha_1[+\eta_2(R_{\rm lo})\sin\theta\,\cos\phi + a_1\eta_1(R_{\rm lo})\cos\theta], \tag{31a}$$

$$\xi_2(R_{\rm lo}) = \alpha_1[-\eta_1(R_{\rm lo})\sin\theta\,\cos\phi + a_1\eta_2(R_{\rm lo})\cos\theta], \tag{31b}$$

$$\xi_3(R_{\rm lo}) = \alpha_2[+\eta_4(R_{\rm lo})\sin\theta\,\sin\phi - a_2\eta_3(R_{\rm lo})\cos\theta], \tag{31c}$$

$$\xi_4(R_{\rm lo}) = \alpha_2[-\eta_3(R_{\rm lo})\sin\theta\,\sin\phi - a_2\eta_4(R_{\rm lo})\cos\theta], \tag{31d}$$

where

$$\alpha_1 = \{[\eta_1(R_{\rm lo})]^2 + [\eta_2(R_{\rm lo})]^2\}^{-1/2},$$

$$\alpha_2 = \{[\eta_3(R_{\rm lo})]^2 + [\eta_4(R_{\rm lo})]^2\}^{-1/2},$$

and

$$a_1 = \frac{\alpha_1}{\sqrt{\alpha_1^2+\alpha_2^2}}, \quad a_2 = \frac{\alpha_2}{\sqrt{\alpha_1^2+\alpha_2^2}}.$$

The angles $\theta$ and $\phi$ in Eq. (31) can assume any values.

With the real and imaginary parts of $v$ defined to be $v^a$ and $v^b$, the currents on $\mathcal{V}_{11}$ and $\mathcal{V}_{22}$ at $R_{\rm lo}$ are

$$j_{v_1}(R_{\rm lo}) = -\frac{1}{M\alpha_1}\sin\theta\,\cos\phi,$$

$$j_{v_2}(R_{\rm lo}) = -\frac{1}{M\alpha_2}\sin\theta\,\sin\phi.$$

We choose to specify $\theta$ and $\phi$ by requiring that the currents at $R_{\rm lo}$ be directed outward, and that their sum be as large as possible. In each instance investigated, $j_{v_2}(R_{\rm lo})$ was found to be vastly smaller than $j_{v_1}(R_{\rm lo})$. It was also found that $j_{v_2}(R_{\rm lo})$ is much smaller than the current $j_{v_2}$ at separations near $R_{\rm hi}$, as ultimately determined after an outward numerical integration.

We now modify our complex wave function. Though this modification has no effect on the relative values of unreflected currents at any separation $R$, the procedure itself proves to be useful in obtaining acceptable expressions for reflected waves. We rewrite $v$ as

$$v = v^a + i f v^b, \tag{32}$$

where $f$ is a complex constant. We determine $f$ by requiring $v$ to resemble a conventional outgoing wave. We are unable to phrase this requirement precisely for a wave whose local wave number does not remain constant, and we look to the WKB approximation for guidance. We require $v$, when integrated outward from $R_{\rm lo}$ to some point $R_s$ where the radial motion of the $\overline{p}$ can reasonably be expected to be more or less semiclassical, to be such that $v_1$ and its derivative satisfy the relation

$$\left.\frac{dv_1}{dR}\right|_{R_s} = \left( ik_1(R_s) - \frac{k_1'(R_s)}{2k_1(R_s)} \right) v_1(R_s), \tag{33}$$

where $k_1$ and $k_1'$ are the local wave number and its derivative on the diabatic surface $\mathcal{V}_{11}$, as specified by

$$k_1(R)=\sqrt{2M[E-\mathcal{V}_{11}(R)]}. \tag{34}$$

Equation (33) is satisfied by a WKB function for outward motion on $\mathcal{V}_{11}$. However, it does *not* lead to a unique specification of $v$ because $f$ then depends somewhat on the choice of $R_s$. It is given by

$$f(R_s)=i\,\frac{\eta_2(R_s)-g_1(R_s)\,\eta_1(R_s)}{\xi_2(R_s)-g_1(R_s)\,\xi_1(R_s)},$$

where

$$g_1(R_s)=ik_1(R_s)-\frac{k_1'(R_s)}{2k_1(R_s)}. \tag{35}$$

Several values of $R_s$ were employed in our numerical calculations. They are

$$R_s^{(1)}=R \quad \text{at first maximum of } |v_1^+|, \tag{36a}$$

$$R_s^{(2)}=R \quad \text{at first node of } v_1^+ \text{ with } R>R_{\rm lo}, \tag{36b}$$

$$R_s^{(3)}=R \quad \text{at first node of } v_2^+ \text{ with } R>R_{\rm lo}, \tag{36c}$$

$$R_s^{(4)}=R \quad \text{at second node of } v_1^+ \text{ with } R>R_{\rm lo}, \tag{36d}$$

$$R_s^{(5)}=R \quad \text{at second node of } v_2^+ \text{ with } R>R_{\rm lo}, \tag{36e}$$

where $v_1^+$ and $v_2^+$ are the components of the real, nearly hydrogenic *regular* solution to Eq. (18) obtained with $E=E^+$. In every instance considered, the real and imaginary parts of $f$ are roughly equal in magnitude, with $10^{-3}\lesssim|f|\lesssim 10^{-2}$. $|f|$ decreases with decreasing angular momentum, but it is fairly insensitive to $R_s$. Our estimated Auger rates prove to be not very sensitive to the choice of $R_s$. (There is no dependence on $R_s$ if the rates are estimated using unreflected currents.) Most of the rates reported in this paper were computed using $R_s^{(2)}$.

### B. Reflected waves on diabatic surfaces

Some of our estimates of Auger rates will be made with waves that have undergone one or more reflections. For this reason we now obtain an inward-traveling wave $v^r$ that can be thought of as being due to the outward-traveling wave $v$ specified by Eq. (32). As with $v$, our expression for $v^r$ is not unique.

In order to specify $v^r$, it is convenient to rewrite our expressions for $v$ and the differential equation that it satisfies. We work with the entirely equivalent relations

$$\zeta=\eta+if\xi, \quad \frac{d\zeta}{dR}=B\zeta,$$

where $\eta$ and $\xi$ are the vector functions defined in Eqs. (29) and (30), $f$ is the complex constant appearing in Eq. (32), and $B$ is an $R$-dependent matrix whose elements are easily obtained from Eq. (18). The complex vector function $\zeta(R)$ specifies the components and derivatives of the complex wave function $v$. It is convenient to write it as

$$\zeta=\sum_{j=1}^{4} a_j\chi^{(j)}, \tag{37}$$

where the $a_j$ are complex constants and the $\chi^{(j)}(R)$ are four suitably chosen, real, linearly independent vector functions, each satisfying the equation

$$\frac{d\chi^{(j)}}{dR}=B\chi^{(j)}.$$

We choose to require the $\chi^{(j)}$ to be orthonormal at $R=R_{\rm lo}$. We also require each component of two of these vectors, $\chi^{(1)}$ and $\chi^{(2)}$, to become vanishingly small as $R\to\infty$. Each component of the two remaining vectors should diverge in this limit. Because our Auger computations are done with $E$ equated to the eigenvalue $E^+$ of Eq. (18), we choose the components of $\chi^{(1)}$ to be proportional to the components and derivatives of the regular solution of this equation with this eigenvalue, as obtained using the procedures outlined in Sec. II D 4. The components of $\chi^{(2)}$ at $R_{\rm lo}$ are equated to expressions almost identical in form to those used in Eq. (31) to specify $\xi(R_{\rm lo})$, the only difference being that the components of $\eta(R_{\rm lo})$ are replaced with those of $\chi^{(1)}(R_{\rm lo})$; and the angles $\theta$ and $\phi$ in these expressions are then adjusted by trial and error until each of the components of $\chi^{(2)}$ vanishes as $R\to\infty$, as determined by numerical integration with $E=E^+$. However, the components of $\chi^{(2)}$, unlike those of $\chi^{(1)}$, presumably all diverge as $R\to 0$. The remaining two vector functions, $\chi^{(3)}$ and $\chi^{(4)}$, whose components presumably all diverge not only as $R\to\infty$ but also as $R\to 0$, are then determined in a straightforward manner by requiring that at $R_{\rm lo}$ both of them be orthogonal to $\chi^{(1)}$ and $\chi^{(2)}$ and also to each other. Once the four orthonormal vectors $\chi^{(j)}(R_{\rm lo})$ are known, the complex coefficients $a_j$ in Eq. (37) are readily determined.

A complex vector function $\zeta^r(R)$ specifying the components and derivatives of the reflected wave $v^r$ is written as

$$\zeta^r=\sum_{j=1}^{4} b_j\chi^{(j)}, \tag{38}$$

where

$$\zeta_1^r=v_1^r, \quad \zeta_2^r=\frac{dv_1^r}{dR}, \quad \zeta_3^r=v_2^r, \quad \zeta_4^r=\frac{dv_2^r}{dR}.$$

The complex coefficients $b_j$ in Eq. (38) are determined by requiring $\zeta^r$ to satisfy appropriate conditions. We require each component of the combined wave function $v+v^r$ to vanish as $R\to\infty$. This leads to

$$b_3=-a_3, \quad b_4=-a_4.$$

The two remaining coefficients, $b_1$ and $b_2$, are determined by requiring $v_1^r$ and $v_2^r$ to resemble inward-traveling WKB functions at some suitable separation. In a manner very similar to our determination of the constant $f$ in Eq. (32), we choose a separation $R_s$, where the relations

$$\left.\frac{dv_1^r}{dR}\right|_{R_s}=\left(-ik_1(R_s)-\frac{k_1'(R_s)}{2k_1(R_s)}\right)v_1^r(R_s), \tag{39a}$$

$$\left.\frac{dv_2^r}{dR}\right|_{R_s}=\left(-ik_2(R_s)-\frac{k_2'(R_s)}{2k_2(R_s)}\right)v_2^r(R_s) \tag{39b}$$

can reasonably be required to be satisfied. The local wave numbers $k_1$ and $k_2$ in Eq. (39) are defined either by Eq. (34) or by

$$k_2(R)=\sqrt{2M[E-\mathcal{V}_{22}(R)]}.$$

The calculation of $b_1$ and $b_2$ then becomes straightforward. Subsequent reflections are taken into account in a similar fashion.

### C. Preliminary expressions for Auger rate

#### *1. In terms of currents on diabatic surfaces*

For reasons presented below, we *tentatively* write a semiclassical estimate of the Auger rate in terms of currents on the diabatic surfaces $\mathcal{V}_{11}$ and $\mathcal{V}_{22}$ as

$$R_A^v=2f_e f_{\bar{p}} f_{\tau_1}\frac{j_{v_2}(R_{\rm hi})}{j_{v_1}(R_{\rm lo})}. \tag{40}$$

The factors $f_e$, $f_{\bar{p}}$, and $f_{\tau_1}$ in Eq. (40) are defined by

$$f_e=4\pi\rho(\epsilon_2),\quad f_{\bar{p}}=\frac{2\pi}{\tau_2},\quad f_{\tau_1}=\frac{2}{\tau_1}, \tag{41}$$

where

$$\rho(\epsilon_2)=\frac{\sqrt{2\epsilon_2}}{(2\pi)^3} \tag{42}$$

and

$$\tau_1=\frac{\pi N^3}{2M},\quad \tau_2=\frac{\pi(N-\Delta N)^3}{2M}. \tag{43}$$

$\tau_1$ and $\tau_2$ are the periods of the $\bar{p}$ for the initial and final states, as calculated with classical mechanics for Kepler orbits with energies

$$E_{N_1}=-\frac{2M}{N^2},\quad E_{N_2}=-\frac{2M}{(N-\Delta N)^2}. \tag{44}$$

$E_{N_1}$ and $E_{N_2}$ are the quantum-mechanical energies of $\bar{p}$ with a principal quantum number $N$ or $N-\Delta N$ bound in a hydrogenic state to an infinitely massive, doubly charged nucleus. Though Eq. (40) proves to be unsatisfactory, it provides a convenient starting point for a more accurate estimate of the Auger rate. The arguments leading to this equation are as follows.

(i) Probability currents can be related to experiment if the motion is nearly classical. To the extent that radial motion of the $\bar{p}$ is indeed nearly classical at separations $R_{\rm lo_+}$ and $R_{\rm hi_-}$ not too far from $R_{\rm lo}$ and $R_{\rm hi}$, and to the extent that the computed currents $j_{v_1}$ and $j_{v_2}$ do not change very much as $R_{\rm lo_+}$ and $R_{\rm hi_-}$ are then allowed to approach $R_{\rm lo}$ and $R_{\rm hi}$, the probability of a transition during the first half-cycle of the $\bar{p}$ orbital motion should be proportional to the ratio of currents in Eq. (40). As explained later, the assumption about motion being nearly classical not too far from $R_{\rm hi}$ is not fully justified for the potentials $\mathcal{V}_{11}$ and $\mathcal{V}_{22}$.

(ii) The factor 2 in Eq. (40) is due to there being two paths possible for a $\bar{p}$ with an angular momentum $L\neq 0$ whose initial radial motion is specified at some point. One path is clockwise, the other counterclockwise. Although we obtained Eq. (18) by assuming that the initial $z$ component of the $\bar{p}$ angular momentum is $+L$, it can also be obtained with $-L$. To put the argument another way, the factor 2 takes into account the fact that Eq. (18) is compatible with the $z$ component of the final electron angular momentum being either $+1$ or $-1$.

(iii) The factor $f_e$ in Eq. (40) is the number of final electron states per unit energy. The need to include $f_e$ in our estimate of the Auger rate arises from an obvious inadequacy of our two-state model: the final electron is in the continuum. (Even with the inclusion of the factor $f_e$, our two-state model is expected to give an acceptable result only if the transition probability is small.) Our expression for $f_e$ follows from the one-to-one correspondence between the **k**-dependent wave functions $\psi_{\rm GR}$ and $\psi_2$ specified in Eqs. (10) and (11). The function $\psi_{\rm GR}$ is normalized to unit density, and in **k** space the number of states in the volume element $d^3\mathbf{k}$ is

$$\frac{d^3\mathbf{k}}{(2\pi)^3}=\rho(\epsilon_2)d\epsilon_2 d\Omega_k,$$

where $\rho(\epsilon_2)$ is defined by Eq. (42) and $d\Omega_k$ is an element of solid angle. For a fixed total energy

$$E=E_{N_2}+\epsilon_2,$$

the final electron energy $\epsilon_2$ is, at least in principle, specified precisely once the final $\bar{p}$ energy $E_{N_2}$ is determined.

(iv) The factor $f_{\bar{p}}$ appears in Eq. (40) because $E_{N_2}$ is determined in practice by a trial-and-error variation of the total energy $E$, with $\epsilon_2$ assumed to be fixed and specified by Eq. (27). In principle, however, $E_{N_2}$ is determined by an integration over a final vibrational quantum number $n_v'$, which can be thought of as varying continuously with an energy $E_{N_2}'$, but which must really be equal to the value $n_v$ specified by Eq. (26). To obtain our expression for $f_{\bar{p}}$, we make use of the relation

$$\delta(n_v'-n_v)=\frac{2\pi}{\tau_2}\delta(E_{N_2}'-E_{N_2}),$$

which is obtained with the aid of the WKB approximation by assuming that the functional dependence of $n_v'$ on $E_{N_2}'$ is given by

$$\left(n_v'+\frac{1}{2}\right)\pi=\sqrt{2M}\int_{R_{\rm lo}}^{R_{\rm hi}}dr\ \sqrt{E'_{N_2}-\frac{(L-\frac{1}{2})^2}{2MR^2}+\frac{2}{R}}.$$

(A somewhat similar procedure is used in the theory of the classical $S$ matrix [3].)

(v) The ratio of currents in Eq. (40) is proportional to a transition probability, but the equation itself specifies a transition rate. This accounts for the presence of the factor $f_{\tau_1}$.

The condition specified in the first of the preceding five arguments is not really satisfied. The wave function $v$ is not a solution of an equation that can be related to truly classical motion at large $R$. If the $\bar{p}$ motion is to be almost classical, it is necessary not only that the local wavelength not be changing too rapidly but also that the coupling with the other state be negligible. As illustrated in Fig. 1, the off-diagonal elements of $\mathcal{V}$ are not truly negligible near $R_{\rm hi}$—in fact, they increase in magnitude with increasing $R$. For this reason we shall modify Eq. (40) so as to use instead a solution of Eq. (23), since its off-diagonal elements, as illustrated in Figs. 4(b) and 4(c), are truly large only within a comparatively narrow range near the avoided crossing. There will still be some difficulty at large $R$, but in Sec. III D we shall attempt to circumvent it, first by evaluating our expression for the current associated with the final state at some suitably chosen radial separation that is in most instances rather smaller than $R_{\rm hi}$, and then by taking into account reflections.

#### *2. In terms of currents on adiabatic surfaces*

The total current, as expressed in Eq. (28), can also be written in terms of a complex solution $w$ to Eq. (23) if the transformation specified by Eq. (21) is employed. It then takes the form

$$j_v=\ j_w=-\frac{i}{2M}\left(w^\dagger\frac{dw}{dR}-\frac{dw^\dagger}{dR}w\right)+\frac{i}{M}\frac{d\Omega_b}{dR}w^\dagger\begin{pmatrix}0&-1\\1&0\end{pmatrix}w.$$

We choose to rewrite this as

$$j_v=j_w=j_{w_1}+j_{w_2},$$

where

$$j_{w_1}=j_{w_1}^{(0)}+j_{w_1}^{(1)},\quad j_{w_2}=j_{w_2}^{(0)}+j_{w_2}^{(1)}$$

and

$$j_{w_1}^{(0)}=-\frac{i}{2M}\left(w_1^*\frac{dw_1}{dR}-\frac{dw_1^*}{dR}w_1\right),\tag{45a}$$

$$j_{w_1}^{(1)}=-\frac{i}{2M}\frac{d\Omega_b}{dR}(w_1^*w_2-w_2^*w_1),\tag{45b}$$

$$j_{w_2}^{(0)}=-\frac{i}{2M}\left(w_2^*\frac{dw_2}{dR}-\frac{dw_2^*}{dR}w_2\right),\tag{45c}$$

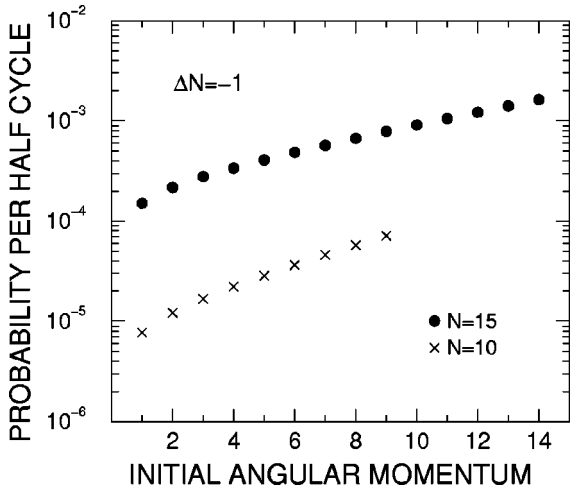


FIG. 5. The Auger transition probability per half-cycle, as obtained by multiplying the transition rate by $\tau_1/2$. The transition rate is computed with the golden rule, and the period of motion $\tau_1$ of the $\bar{p}$ in the initial state is computed with classical mechanics.

$$j_{w_2}^{(1)}=+\frac{i}{2M}\frac{d\Omega_b}{dR}(w_2^*w_1-w_1^*w_2).\tag{45d}$$

The expressions for $j_{w_1}^{(0)}$ and $j_{w_2}^{(0)}$ are identical in form to those for $j_{v_1}$ and $j_{v_2}$. The terms $j_{w_1}^{(1)}$ and $j_{w_2}^{(1)}$—which are equal to each other—are due to the presence in Eq. (23) of a first derivative of $w$. Assigning half of their sum to each of our expressions for the currents on $\mathcal{W}_+$ and $\mathcal{W}_-$ is admittedly arbitrary, but it proves to be of little importance in estimating Auger rates.

An Auger transition occurs if the outward moving $\bar{p}$ remains on the adiabatic potential surface $\mathcal{W}_+$. For this reason we now write down *another tentative estimate* of the transition rate. This estimate is

$$R_A^w=2f_ef_{\bar{p}}f_{\tau_1}\frac{j_{w_1}(R_{\rm hi})}{j_{w_1}(R_{\rm lo})},\tag{46}$$

where the factors $f_e$, $f_{\bar{p}}$, and $f_{\tau_1}$ are the same as before, but $R_{\rm lo}$ and $R_{\rm hi}$ are now lower and upper bounds of the range of separations for which classical motion is allowed on the upper adiabatic surface. The important difference between Eqs. (40) and (46) is the difference between $j_{v_2}(R_{\rm hi})$ and $j_{w_1}(R_{\rm hi})$, which can be considerable.

In Eq. (46), as in Eq. (40), we have not taken into account reflections of the outgoing wave. To put the matter another way, we have taken into account only one of the many opportunities that $\bar{p}$ has to remain on an adiabatic surface. In each of the instances considered in the present paper, a $\bar{p}$ initially on one adiabatic surface is very unlikely to remain on that surface as it passes the avoided crossing. This is illustrated in Fig. 5, which shows the Auger transition probability per half-cycle, as obtained from our golden rule calculations by multiplying the transition rate by $\tau_1/2$. This figure shows that a transition becomes likely to have occurred only after there have been many encounters of the $\bar{p}$ with the crossing. Nevertheless, using Eq. (46), or some variation

thereof, would appear to be a reasonable procedure, since the many contributions to the transition amplitude, each associated with one such encounter, should contribute incoherently to the rate because of phase differences. The matter of phase differences and incoherence will be discussed in Sec. III E.

The preceding arguments notwithstanding, there is still a problem with Eq. (46). The difficulty is due to the presence of some not entirely negligible, velocity-dependent, off-diagonal terms in Eq. (23) at large $R$. A very rough approximation to the magnitude of these terms is shown in Fig. 4(b) for a traveling wave. As explained in more detail later, in Sec. III D, these terms are responsible in some instances for a troublesome increase in probability current at large $R$ that ultimately is of little or no consequence.

#### *3. In terms of probabilities rather than currents*

To the extent that our model is valid, Auger rates should also be expressible in terms of time-dependent probabilities. It should suffice to determine the time-dependent probability of the $\bar{p}$ being in the upper or the lower component of a suitably specified approximate solution $u$ of Eq. (14).

We obtain an estimate by assuming that at time $t=0$, the $\bar{p}$ is initially in the nonstationary state

$$u_i(R)=\frac{1}{\sqrt{2}}[u^+(R)+u^-(R)],$$

where $u^+$ and $u^-$ are the linearly independent regular solutions of Eq. (14) with slightly different eigenvalues $E^+$ and $E^-$, as discussed in Sec. II D 4. To a very good approximation, $u_i$ has appreciable amplitude only for the upper component of $u$. The probability at some later time $t$ of the $\bar{p}$ being in the nonstationary state $u_f$, defined by

$$u_f(R)=\frac{1}{\sqrt{2}}[u^+(R)-u^-(R)],$$

is given exactly by

$$P_f(t)=\sin^2\left(\frac{(E^+-E^-)t}{2}\right).$$

To a very good approximation, $u_f$ has appreciable amplitude only for the lower component of $u$. As long as the probability of the $\bar{p}$ being in the initial state $u_i$ remains nearly equal to unity—and to the extent that our model is valid—the Auger rate should be given approximately by

$$R_A=2f_e f_{\bar{p}}^- \frac{1}{t}P_f(t),$$

where $f_e$ and $f_{\bar{p}}^-$ are defined in Eq. (41). Our reasons for the factors 2, $f_e$, and $f_{\bar{p}}^-$ in the preceding equation are the same as they are for Eq. (40).

If $P_f \ll 1$, our expression for $R_A$ varies linearly with $t$. It is, therefore, generally incorrect, which implies that our model—or, at the very least, some of the results obtained with it—must be modified. The same difficulty is encountered in Sec. III D 2, where estimates of the Auger rate are computed using probability currents for reflected and multiply reflected waves.

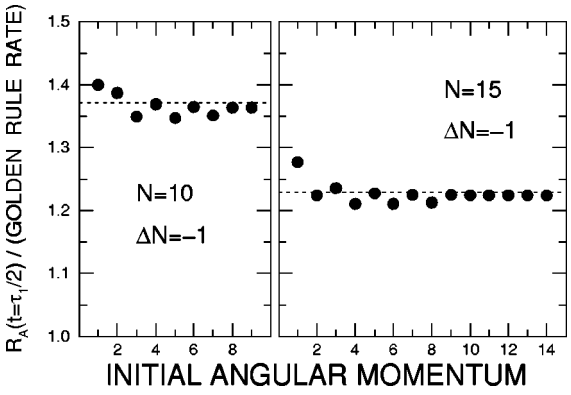


FIG. 6. The ratio of the rate $R_A$, evaluated at time $t=\tau_1/2$, to the Auger rate computed using the golden rule. The dotted lines show the values of $\tau_1/\tau_2$. $\tau_1$ and $\tau_2$ are the periods of the initial and final states, as computed with classical mechanics.

Probabilities varying quadratically with $t$ are also obtained with time-dependent perturbation theory. This is, of course, a feature of some derivations of the golden rule. In the case of the golden rule, this difficulty can be circumvented [29]. It is also possible to circumvent it in the case of $R_A$. As explained below, nearly exact agreement with numerical results obtainable for $\bar{p}\mathrm{He}^+$ by using the golden rule should also be obtainable with our model—though in a not especially elegant way—by (i) allowing $N$ and $M$ to become sufficiently large, (ii) discarding all values of $R_A$ *except* the one for $t=\tau_1/2$, (iii) then considering times that are not only large enough to ensure that many half-cycles of (almost classical) $\bar{p}$ motion have occurred but are also small enough to ensure that the initial state remains largely undepleted, and (iv) simply *assuming* that the separate contributions to the *actual* time-dependent transition amplitude from the many half-cycles of $\bar{p}$ motion not only have magnitudes that are all nearly equal to the magnitude of the amplitude leading to our value of $R_A$ at $t=\tau_1/2$ but also have phases that are *somehow* effectively random, thereby permitting the cross terms in the absolute square of the amplitude to be neglected.

Our assertion of being able to achieve nearly exact agreement with the golden rule is based on Fig. 6, which shows the ratio of $R_A$, as evaluated at $t=\tau_1/2$, to the golden rule rate. $R_A$ was computed by first setting $f_r=0.01$ and then dividing the result by $f_r^2$. (It will be recalled from Sec. II D 4 that the small energy difference $E^+-E^-$ is very nearly proportional to the multiplicative factor $f_r$.) Our values of $R_A$ differ from the golden rule rate by a factor not very different from unity. In every instance this factor is nearly equal to $\tau_1/\tau_2$. Therefore, nearly exact agreement with the golden rule should be achieved if $N$, as it appears in the expressions for the periods $\tau_1$ and $\tau_2$ given by Eq. (43), is allowed to become very large. (If agreement with the golden rule is to be achieved by allowing $N$ to become very large, while retaining our original assumptions that (i) the mean orbital radius of the $\bar{p}$ is much less than that of the electron, and (ii) the spacing between adjacent principal levels of the $\bar{p}$ is

large enough to permit Auger ejection, it would also be necessary to think of $M$ as being much larger.)

### D. Numerical results

#### 1. Estimates with unreflected waves

Figure 7 shows the unreflected current $j_{w_1}$ on the upper adiabatic surface at radial separations in the range $R_{\rm lo}<R<R_{\rm hi}$. This current was calculated in each instance with $f_r=0.01$. It is shown on two scales because it changes very rapidly near the avoided crossing. The unreflected current $j_{w_2}$ on the lower surface is also shown, but only at separations below the crossing. Using a different value of $f_r$ would cause both currents to change, though their sum would remain constant. However, except at separations so near the crossing as to be practically invisible on the scales used in Fig. 7, these changes can be specified rather accurately in terms of the currents obtained with $f_r=0.01$. In the case of $j_{w_1}$ there would be no visible dependence on $f_r$ below the crossing, while at all separations perceptibly beyond this point the current would be almost precisely proportional to $f_r^2$. The current $j_{w_2}$ shown in Fig. 7 for separations below the crossing is also very nearly proportional to $f_r^2$. (It was found in all of our calculations, including those involving reflected waves, that the current assumed to be proportional to the Auger rate is almost exactly proportional to $f_r^2$.) Unless $L$ is relatively large, $j_{w_1}$ has a minimum at a separation between the crossing point and $R_{\rm hi}$. This minimum, which is marked in Fig. 7, occurs at the same radial separation where the angle $\Omega_b$ specified by Eq. (22) has a minimum, as shown in Fig. 3(b). This separation will be denoted by $R_b$. Since the velocity-dependent coupling term in Eq. (23) vanishes at $R_b$, the $\overline{p}$ motion at this point should be almost classical if the local wavelengths on both adiabatic surfaces are not changing too rapidly. In those instances where $j_{w_1}$ has no minimum below $R_{\rm hi}$, we simply define $R_b$ to be equal to $R_{\rm hi}$. The increase in $j_{w_1}$ at separations beyond $R_b$, which is quite small if $L$ is large, becomes relatively large as $L$ decreases. For example, the ratio of $j_{w_1}$ at $R_{\rm hi}$ to its value at $R_b$ for the transition from the state with $N=15$ and $L=1$ is $\sim 7$. These increases in $j_{w_1}$ are troublesome because Eq. (46), without further modification, would lead to an unacceptable overestimate of the Auger rate in many instances. However, these overestimates would be of little significance because, as explained in Sec. III D 2, once a reflection is taken into account, the increase in $j_{w_1}$ at large separations—or much of it—has no lasting effect.

Figure 8 shows the ratio of the Auger rate $R_A^w$, as computed using a *modification* of Eq. (46), to the rate obtained using the golden rule. The modification is that the unreflected current $j_{w_1}$ in the numerator of Eq. (46) is evaluated at $R_b$ rather than $R_{\rm hi}$. Except for transitions between orbitals with fairly small or very large angular momenta, the agreement between the two rates is good, in most instances very good, but we acknowledge that further justification should be provided for ignoring the (sometimes relatively large) increases in $j_{w_1}$ at classically allowed separations beyond $R_b$. At first glance it might seem that the lack of agreement at

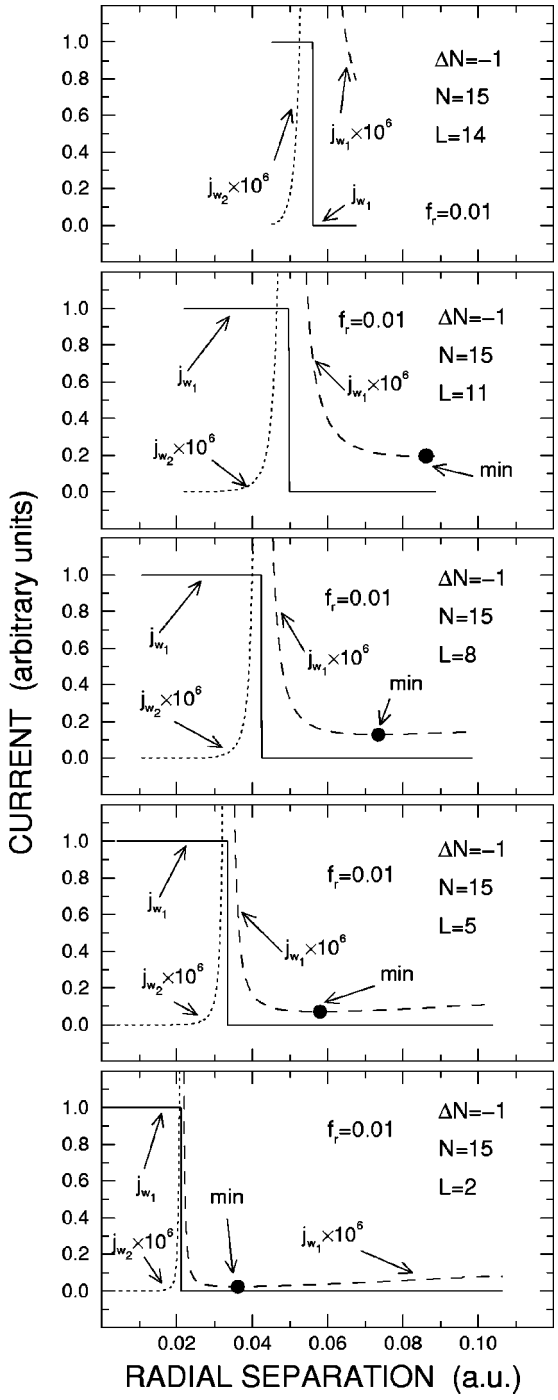


FIG. 7. The unreflected current $j_{w_1}$ at radial separations where motion is classically allowed on both the upper and lower adiabatic surfaces. The unreflected current $j_{w_2}$ is also shown, but only at separations below the crossing point. The minimum of $j_{w_1}$ is marked in every instance where it occurs below the upper bound for classical motion.

both fairly small and very large $L$ would be due to inadequacy of the arguments leading to our original expression for $R_A^w$, but, as argued in Sec. III D 2, it seems more likely at fairly small $L$ that this is simply due to $R_b$ not always being a suitable point to evaluate $j_{w_1}$. It must be added that the ratios of rates shown in Fig. 8 are not changed much if $j_{w_1}$ is approximated by $j_{w_1}^{(0)}$, as specified by Eq. (45a): the changes

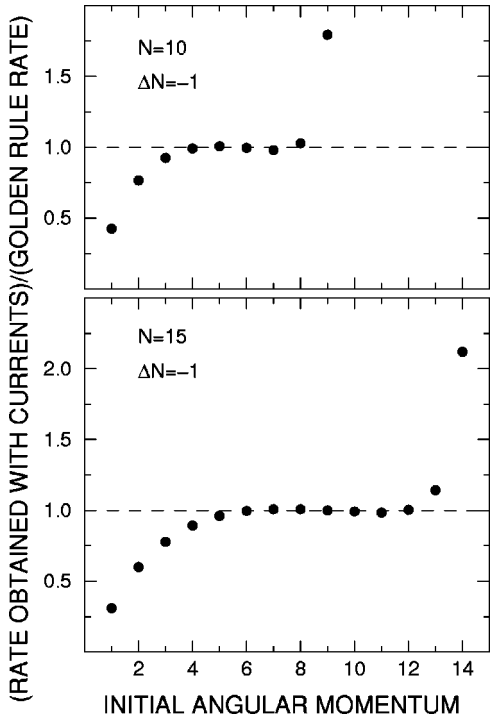


FIG. 8. The ratio of the Auger rate $R_A^w$, as computed using the unreflected current $j_{w_1}$ on the upper adiabatic surface at $R_b$ rather than $R_{\rm hi}$, to the rate computed using the golden rule.

are less than 1%, usually much less, except for circular or nearly circular orbits, in which case the ratios become as much as 13% smaller.

The question arises as to whether accurate rates could be obtained by using currents on the diabatic surfaces. Such rates would be specified by Eq. (40) or some reasonable modification thereof. Since the outgoing currents $j_{w_1}$ and $j_{v_1}$ are practically identical at $R_{\rm lo}$ if $L$ is not too high, the adequacy of this equation should be revealed by the relative differences between $j_{w_1}$ and $j_{v_2}$ at large separations. A detailed investigation of this question has shown that satisfactory overall agreement with the golden rule could not be achieved if unreflected currents on the diabatic surfaces were to be employed, no matter where $j_{v_2}$ would be evaluated. This conclusion is not surprising: the fundamental nature of the adiabatic representation in reactions involving electronic rearrangement has long been recognized [21]. (A similar conclusion does not apply to some of the estimates presented in Sec. III D 2, because the inward traveling currents $j_{w_2}$ and $j_{v_2}$ are very nearly the same at $R_{\rm lo}$ if $L$ is not too high.)

Figure 9 shows some radial separations relevant to the transitions being considered. It shows the lower and upper classical turning points $R_{\rm lo}$ and $R_{\rm hi}$, approximate bounds of the transition region, and the location of the avoided crossing. The approximate bounds of the transition region are defined arbitrarily to be the lowest separations where $j_{w_2}$ and $j_{w_1}$ are equal to twice the value of $j_{w_1}$ at $R_b$. These approximate bounds are unaffected by the choice of the multiplicative factor $f_r$. We argue that the results in this figure, together with those in Figs. 7 and 8, suggest that an Auger transition can be thought of as occurring on an adiabatic surface at a relatively well defined radial separation.

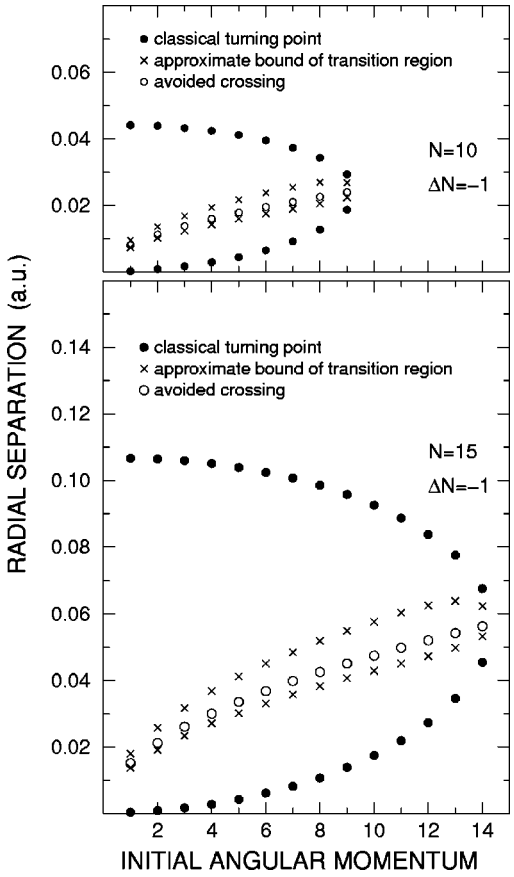


FIG. 9. The classical turning points, approximate bounds of the transition region, and the location of the avoided crossing for transitions with $\Delta N=-1$ from states with $N=10$ or 15.

Good agreement with golden rule rates notwithstanding, our procedure clearly demands more scrutiny, if only because our largely *ad hoc* modification of Eq. (46) might never have been introduced had it not been for the troublesome increases in $j_{w_1}$ for small $L$ and large $R$ evident in Fig. 7. There is, however, a second reason. In some instances the $\overline{p}$ motion at $R_b$ is not semiclassical, which makes it awkward to relate $j_{w_1}$ to experiment. This is obviously the case in those instances where $R_b=R_{\rm hi}$. It is also the case in a few other instances, where the classical action on the corrected upper adiabatic surface, as computed between $R_b$ and $R_{\rm hi}$, is quite small. Therefore, rates were also estimated using reflected waves, together with further modification of Eq. (46).

#### *2. Estimates with reflected waves*

Some results obtained with reflected waves are shown in Fig. 10. This figure, like Fig. 8, shows ratios of $R_A^w$ to golden rule rates. However, in obtaining the ratios in Fig. 10, the current in the numerator of Eq. (46) was replaced with a current computed with a reflected or multiply reflected wave that had experienced two, three, or four encounters with the avoided crossing. This current is *tentatively* assumed to be proportional to the probability that a transition occurs at some time during the first two, three, or four half-cycles of $\overline{p}$ motion. Because of the longer periods of time, the expression for $R_A^w$ was again modified: it was decreased by a factor equal to the number of half-cycles. The reflected waves and

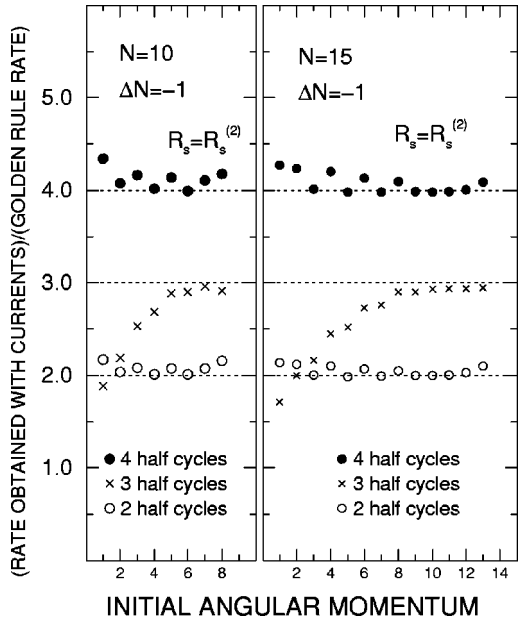


FIG. 10. The ratio of the Auger rate $R_A^w$, as computed using radial waves that have been reflected one, two, or three times, to the rate computed using the golden rule.

the currents associated with them were calculated using the procedures outlined in Secs. III B and III C. The former procedure requires the aid of the WKB approximation at some suitable separation $R_s$ to ensure, as much as we are able within the framework of our model, that a reflected wave is going in the desired direction. The ratios shown in Fig. 10 were all obtained using $R_s^{(2)}$, as specified by Eq. (36b). If the number of half-cycles was even, the already twice modified Eq. (46) was modified again by replacing the current in its numerator with the inward-traveling current $j_{w_2}$ on the lower adiabatic surface at $R_{\rm lo}$. Except for transitions from nearly circular orbitals, $j_{w_2}$ was found to be almost constant throughout an interval between $R_{\rm lo}$ and some nearby point that is not only well below the lower bound of the transition region shown in Fig. 9 but also such that the WKB approximation should be fairly reliable. Therefore, in most instances there would appear to be no serious problem in relating $j_{w_2}(R_{\rm lo})$ to experiment, even though the $\overline{p}$ motion is not semiclassical at $R_{\rm lo}$. In the case of three half-cycles the outward moving current in the numerator of Eq. (46) was evaluated, as before, on the upper adiabatic surface at $R_b$. The results shown in Fig. 10 are *not* in agreement with the golden rule, and it is the aim of the discussion presented in Sec. III E to reconcile the two calculations.

The most striking feature of Fig. 10 is that the ratio of rates is in many instances roughly equal to the number of half-cycles. This is generally true if the number of half-cycles is even. However, it is not true of the ratios for three half-cycles if $L$ is relatively low. The overall behavior of the ratios for three half-cycles in Fig. 10 more or less resembles that for a single half-cycle in Fig. 8. In both figures the ratio is nearly equal to the number of half-cycles if $L$ is large (except for circular orbitals, which are shown only in Fig. 8), but it becomes much smaller as $L$ becomes small. Because of the near constancy of the ratios for two and four half-cycles, even if $L$ is low, we suspect that these decreases are due not so much to inadequacy of the arguments leading to our original expression for $R_A^w$ as they are to $R_b$ simply not always being an appropriate choice of separation to evaluate $j_{w_1}$ for the final state.

A simple, classical argument lends qualitative support to our suspicion that $R_b$ is not always a suitable place to evaluate $j_{w_1}$ in a rate estimate. If the FCP is to be satisfied, an Auger transition should be inhibited at any separation where there would be a relatively large change in the local, classically computed radial momentum. A straightforward calculation has shown that, while $R_b$ would indeed appear to be an acceptable lower bound in many instances to the range of large, classically allowed separations where the radial momenta on the two adiabatic surfaces are comparatively different, a more realistic lower bound to this range would be appreciably greater than $R_b$ if $L$ is fairly low. We therefore believe that there is some physical justification for discarding the ratios for low $L$ shown in Fig. 8 in favor of ratios obtained with $j_{w_1}$ evaluated at somewhat higher separations. An examination of Figs. 7–9 indicates that this would not require abandoning our interpretation of the transition as occurring within a range of separations small compared to the classically allowed range. Similarly, for waves that have been reflected twice, the discrepancies with the golden rule, as shown in Fig. 10, could be made more nearly a uniform factor $\sim 3$.

Complications of the sort encountered at large separations do not arise if the number of half-cycles is even, and because of this we conclude that the relatively small deviations of the ratios in Fig. 10 from 2.0 and 4.0 for two and four half-cycles are largely a consequence of our use of the WKB approximation at some separation $R_s$ on the diabatic surfaces to determine that waves are proceeding in the proper direction on the adiabatic surfaces. We believe that this conclusion is supported (to some extent) by ratios computed, when possible, with each of the five choices of $R_s$ listed in Eq. (36). Results were obtained for transitions from states with $N=15$ and $L=2$, 5, 8, 11, 13, or 14, in each instance for two half-cycles. Except for the transition between circular orbitals—for which our only value of $R_s$ is *beyond* the crossing point and is, therefore, not really an appropriate place to determine that on both surfaces the reflected wave is indeed moving inward at points near $R_{\rm lo}$—the deviations of these ratios from 2.0 were found to have the same magnitude and usually the same sign as the relatively small deviations shown for two half-cycles in Fig. 10.

It seems clear from some of the results shown in Figs. 7–10 that the net effect of an inward traversal of the crossing is that much, if not all, of any troublesome increase in $j_{w_1}$ at large separations has no lasting effect, probably because of the relatively large momentum changes that must accompany transitions occurring at separations much beyond the crossing. Because of the results shown in these figures, and also because of investigations by others which have shown that some chemical reactions can be understood in terms of almost classical trajectories on adiabatic surfaces [3,20,21], we conclude that the time-dependent amplitude for an Auger transition can be thought of as a sum of contributions, each associated with a radially rather well defined encounter with

the avoided crossing during which the $\bar{p}$ remains on the same adiabatic surface instead of hopping to the other one. However, the large and more or less regular discrepancies with the golden rule for rates computed with reflected waves must still be resolved.

### E. Phase differences

It is apparent from Fig. 10 that fairly good agreement with the golden rule would be achieved if some reason could be found for dividing each of the ratios in this figure—modified in some instances by using an outgoing current evaluated at a separation somewhat greater than $R_b$—by the number of half-cycles. We can think of no reason why this would be justified after only a small number of half-cycles. However, as indicated in Fig. 5, many half-cycles are required before a transition becomes likely to have occurred. If, as we have concluded, the time-dependent transition amplitude is a sum of contributions from many radially rather well defined encounters of the $\bar{p}$ with the avoided crossing, and if these many contributions all have nearly the same magnitude but effectively random phases, the cross terms in the absolute square can reasonably be expected to have no net effect. In Sec. III E 4 we shall argue that this would likely be the case if the finite width of the initial state were to be taken into account. Our arguments will be based on some estimates of phase differences due to radial motion. But before that, in Sec. III E 3, we shall discuss a possible phase difference due to angular motion that can be estimated using classical orbits (which will be discussed in Sec. III E 2), *and we shall conjecture that it might be important in the special type of Auger transition which occurs during EAF*. This phase difference is the angular analog of what we shall refer to as the traditional Stückelberg phase, which is associated with radial motion, and which is defined and discussed below.

#### *1. Traditional Stückelberg phase*

In obtaining the ratios shown in Figs. 8 and 10 we have in effect assumed that a current, either $j_{w_1}(R_b)$ directed outward or $j_{w_2}(R_{\rm lo})$ directed inward, is proportional to the absolute square of the amplitude for the occurrence of a transition at some time during a certain number of half-cycles. Our results imply that the contributions of each half-cycle have not only nearly the same magnitude but also nearly the same phase. This near equality of phase merits discussion, if only because we have really been treating a $\bar{p}$ Auger transition as a LZS process. It was at one time widely accepted that the two contributions to the amplitude for a LZS transition of the usual kind (inelastic scattering) should differ in phase by an amount related in a simple fashion to the difference in radial action along the two possible classical paths between the encounters with the avoided crossing. We shall refer to this phase difference as the traditional Stückelberg phase. For the transitions being considered here, it is readily estimated using unperturbed Coulomb potentials, and in most instances its effect is not negligibly small. Our failure to achieve agreement with the traditional Stückelberg phase is, by itself, unremarkable because it has been known for some time that the traditional LZS formula [30] leads to incorrect results in some instances [31], including those in which the transition probability is small [32]. *We call attention to this lack of agreement because in Sec. III E 3 we shall conjecture that the angular analog of the Stückelberg phase, as estimated in the traditional way, might be important in EAF*.

Even though the lack of agreement with the traditional LZS formula is unsurprising, we can only hazard a guess as to why our estimated contributions to the transition amplitude are so nearly equal in phase. As suggested by the results of an approximate calculation sketched in the next paragraph, differences in the radial action should indeed be important. Therefore, it would seem that there must be some mechanism that has nearly the opposite effect as the difference in radial action. We suspect that this mechanism is associated in some way with one or both of the off-diagonal terms in Eq. (23), which take into account all coupling between the initial and final states due to both radial and angular motion. Because all coupling due to angular motion is taken into account in the radial wave equation, we shall assume in Sec. III E 3 that there is no mechanism that would diminish a similar difference in angular action, as estimated in the traditional way.

The traditional Stückelberg phase can be made to appear in an *approximate* golden rule expression. The derivation is similar to that of an approximate expression for the Franck-Condon factor given by Miller [33]. It is only necessary that the $\bar{p}$ radial dipole matrix element not be computed exactly but instead be roughly estimated by first replacing the initial and final hydrogenic wave functions with WKB functions and then using the stationary phase approximation to evaluate the integral. The form of the resulting approximate expression for the transition rate is proportional to the traditional LZS formula, which contains the factor

$$f_S=\cos^2\left(\phi_2-\phi_1-\frac{\pi}{4}\right),$$

where $\phi_1$ and $\phi_2$ are the integrals of the local radial wave numbers for the initial and final unperturbed states from the lowest classical turning points to the crossing point. Because of the preceding expression, we choose to define the traditional Stückelberg phase as

$$\phi_S=2(\phi_2-\phi_1)-\frac{\pi}{2}. \tag{47}$$

The absolute square of the sum of two amplitudes, equal in magnitude but differing in phase by $\phi_S$, would be proportional to $f_S$. We note that an implicit appearance of this factor in our estimates of Auger rates using probability currents would have been unwelcome. A straightforward calculation indicates that the presence of $f_S$ would cause the estimated transition rate to depend on the $\bar{p}$ angular momentum in a way quite different from the dependence obtained with the presumably accurate golden rule, as shown in Fig. 5. Our failure to achieve agreement with the traditional Stückelberg phase is almost surely associated with the breakdown of the WKB approximation near the avoided crossing.

### 2. Relating $\bar{p}$ wave functions to classical orbits

The FCP should still hold for motion in more than one dimension: it should still be possible to think of a transition amplitude as being a sum of contributions, each produced near a point where both the radial separation and the radial momentum are the same in the initial and the final states. We denote this separation by $R_c$. To gain some insight into this matter, we examined some classical orbits. We assumed that infinite manifolds of coplanar Kepler orbits with energies given by Eq. (44) adequately describe the initial and the final motion of the $\bar{p}$. As in our quantum-mechanical calculations, it was assumed that the squares of the initial and the final angular momenta are $L(L+1)$ and $(L-1)L$. If the effective radial potential for the final orbit is increased by an amount equal to the increase in binding energy of the $\bar{p}$, it intersects the effective potential for the initial orbit at the separation $R_c$. Two coplanar orbits with suitably different energies and angular momenta intersect at the required separation $R_c$ if they are properly oriented with respect to each other. For a given initial (final) orbit, two orientations are possible for a final (initial) orbit. For one of the orientations, radial motion on both orbits proceeds inward toward the nucleus at the intersection; and for the other, motion proceeds outward.

Figure 11(a) shows both possible orientations of a final orbit with $N=14$ and $L=7$ with respect to an initial orbit with $N=15$ and $L=8$. All of the orbits lie in the $x$-$y$ plane. All points on the two final orbits a distance $R_c$ from the nucleus are marked, even if they are not located at an intersection with the particular initial orbit we have chosen to show. Motion on each of these orbits is regarded as proceeding counterclockwise. We define $\Phi_1^{\rm in}$ ($\Phi_1^{\rm out}$) to be the angular position of the point on the initial orbit with separation $R_c$ and inward (outward) radial motion, and we also define

$$\Delta\Phi_1=\Phi_1^{\rm out}-\Phi_1^{\rm in}.$$

The angles $\Phi_2^{\rm in}$, $\Phi_2^{\rm out}$, and $\Delta\Phi_2$ are similarly defined for a final orbit. The magnitude of the angular separation between the two final orbits in Fig. 11(a) is $\Delta\Phi_2-\Delta\Phi_1$. (If we had instead shown just one final orbit and the two possible initial orbits associated with it, the magnitude of the angle between the two initial orbits would also have been $\Delta\Phi_2-\Delta\Phi_1$.) Figure 11(b) shows $\Delta\Phi_1$ and $\Delta\Phi_2$ for all of the transitions being considered. *These angles are large, and they have a significant dependence on angular momentum. This will lead us to conjecture in Sec. III E 3 that, because of differences in angular motion, interference between two contributions to the transition amplitude could be important in EAF.*

It is necessary to be more precise about how we relate wave functions to classical orbits. To be specific, we consider a hydrogenic state with principal quantum number $N$ and angular momentum $L$. As in Sec. II A, we assume that the $z$ component of the angular momentum is $L$. For the time being, we also assume that this state is not coupled to any other state. We first write the wave function in the usual way as

$$\mathcal{R}_{N,L}(R)Y_{L,L}(\Theta,\Phi),$$

where $\mathcal{R}_{N,L}$ is real. We assume that $N$ is large and $L$ is not small. The radial motion is almost classical except near the turning points, and the azimuthal motion is almost classical everywhere. Furthermore, the motion is almost two dimensional because $Y_{L,L}$ has appreciable amplitude only in the neighborhood of the $x$-$y$ plane. It is convenient to express the radial function approximately as the sum of two waves, outward motion with one and inward with the other:

$$\mathcal{R}_{N,L}(R)\approx\chi_{N,L}^{(+)}(R)+\chi_{N,L}^{(-)}(R).$$

We accomplish this by replacing $\mathcal{R}_{N,L}$ with a suitably chosen real function and then adding and subtracting a suitably chosen imaginary function. We shall assume that $\chi_{N,L}^{(+)}$ and $\chi_{N,L}^{(-)}$ are WKB functions.

For the moment, we restrict our attention to the wave

$$\chi_{N,L}^{(+)}(R)Y_{L,L}(\Theta,\Phi),$$

which is simultaneously proceeding radially outward and azimuthally counterclockwise. At any given point where the radial motion is almost classical, the phase of this wave can be identified with Hamilton's characteristic function $W_0$ for classical motion passing through this point, with $\nabla W_0$ being

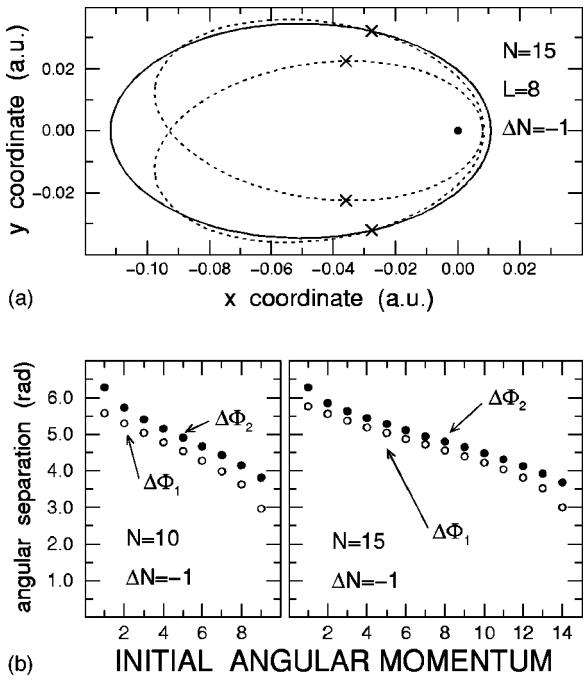


FIG. 11. Results of calculations using classical mechanics and Kepler orbits, but with quantum-mechanical values for the energies and the squares of the angular momenta. (a) One of the initial orbits and two of the final orbits relevant to the transition with $\Delta N=-1$ from the state with $N=15$ and $L=8$. The nucleus is at the origin, and the initial orbit (solid line) has its major axis parallel to the $x$ axis. The two final orbits (dotted lines) are the only ones that intersect the initial orbit at a point where the FCP is satisfied. These intersections occur at a distance $R_c$ from the nucleus. The two points on each orbit a distance $R_c$ from the nucleus are marked; but on a given final orbit, one of these points is at an intersection with an initial orbit that is not shown. (b) The angular separations $\Delta\Phi_1$ and $\Delta\Phi_2$ on the initial and final orbits between two successive encounters of the $\bar{p}$ with separations a distance $R_c$ from the nucleus. The radial motion is assumed to be directed inward during the first encounter.

the momentum **P** along a locally well defined trajectory [34]. For a fixed value of $\Phi$, there is a different trajectory associated with each value of $R$ where motion is almost classical. Motion on each of these trajectories has the same total energy, but the momentum **P** has a momentary value depending on $R$. We shall think of each of these trajectories as being in the $x$-$y$ plane. By the nature of the WKB approximation, the difference in phase of $\chi^{(+)}_{N,L}Y_{L,L}$ at any two points lying along a given orbit is given by the integral $\int \mathbf{P}\cdot d\mathbf{R}$ along the segment of orbit connecting them, provided this segment does not include any points where motion is not almost classical. This integral is the sum of two terms, the radial and the angular action along the segment.

In a manner similar to the way we relate $\chi^{(+)}_{N,L}Y_{L,L}$ to classical trajectories, we also associate

$$\chi^{(-)}_{N,L}(R)Y_{L,L}(\Theta,\Phi)$$

with a manifold of locally well-defined trajectories, all moving azimuthally counterclockwise, but radially inward. Both radial waves $\chi^{(+)}_{N,L}$ and $\chi^{(-)}_{N,L}$ can be thought of as ultimately undergoing reflection at a classical turning point, thereby being turned in to each other in the usual way of WKB functions. For this reason, the outgoing (ingoing) local trajectory for given values of $R$ and $\Phi$ can be associated with the ingoing (outgoing) local trajectories for *other* combinations of $R$ and $\Phi$ to form parts of a continuous orbit. There would be a nondenumerably infinite number of such orbits, all proceeding counterclockwise, and with orientations distributed uniformly in the $x$-$y$ plane. For every value of $\Phi$, there would be two of these orbits passing through every point specified by a classically allowed value of $R$, one with motion directed inward, the other with motion outward. By making use of the usual procedures for determining reflections of WKB waves, we can assign a well-defined phase difference between *any* two points on a given orbit—even if all of the segment of orbit connecting them does not lie in the region where quantum-mechanical motion is almost classical—provided the two points themselves do lie in this region. The angular contribution to this phase difference is $L\Delta\Phi$, where $\Delta\Phi$ is the angular separation between the two points. While the preceding discussion has been devoted to a hydrogenic function, most of it also applies to a similarly specified wave function for almost classical motion in any central field, the essential difference being that the classical orbits would generally not be closed, as they would be for a hydrogenic function with large $N$ and $L$.

#### *3. Possible phase difference due to angular motion on different paths*

The numerical results presented in Figs. 1 and 3 and Eqs. (19) and (20) indicate that the successive transformations $U_a$ and $U_b$ relating the radial functions $u_1$ and $u_2$ appearing in Eq. (1) to the functions $w_1$ and $w_2$ in Eq. (21) are such that the angular momenta on the two paths between encounters with the avoided crossing effectively differ by $\sim 1$ unit, except near the crossing. As outlined below, a difference in angular action—which has not been taken into account in our Auger calculations using the modern BO approximation and probability currents—could reduce constructive interference substantially. By angular action we simply mean that contribution to the integral $\int \mathbf{P}\cdot d\mathbf{R}$ along the (almost classical) trajectory of the $\overline{p}$ which is due to components of the momentum **P** orthogonal to the radius vector from the origin.

We are interested in the effects that phase differences might have on Auger transition probabilities. This involves motion on two coupled adiabatic surfaces. As already discussed in considerable detail, we argue that transitions can be thought of as occurring near radial separations where $R = R_c$, in accord with FCP. The WKB approximation for radial motion breaks down near such points. For this reason, semiclassical estimates of phase differences between points on a path corresponding to a transition should be unreliable. We shall assume that our quantum-mechanical computations of the radial phases, as presented later, in Sec. III E 4, are reliable. *But because the off-diagonal elements of (the radial wave) Eq. (14) already take into account all coupling due to angular motion, and also because currents computed using the radial wave function w obtained by successive unitary transformations from the function u appearing in Eq. (14) lead to rather good agreement with the golden rule if only a single traversal of the avoided crossing is taken into account, we shall further assume that reliable estimates of phase differences due to angular motion can be obtained by simply computing the angular action along the appropriate segments of classical orbits*.

If the perturbation responsible for transitions is taken into account—and if we think in terms of classical paths—the FCP would require each path associated with the initial state to spawn a path associated with the final state every time it passes a point with the radial separation $R_c$. Each path, including those originating with a transition, would have associated with it a phase that is continually increasing as the motion proceeds. As outlined below, we argue that there could be significant differences in phase between different paths leading to a given final orbit.

In what follows, we shall consider waves moving (effectively in two dimensions) on adiabatic surfaces that have fairly well-defined angular momenta, except near the avoided crossing. We shall restrict our attention to the phase difference associated with just two successive encounters with the crossing. Furthermore, we shall consider only the phase difference associated with angular motion. We shall assume that the first encounter occurs as the motion proceeds inward, the second as it proceeds outward. Except for the absence of a term $-\pi/2$, which arises in the reflection of a WKB radial wave, the phase difference would be the angular analog of the traditional (radial) Stückelberg phase $\phi_S$, as we have defined it in Eq. (47).

In estimating the phase difference due to angular motion, we consider three Kepler orbits more or less similar to those shown in Fig. 11(a), the difference being that we now consider two initial orbits and just one final one, not the other way around. However, even though it is convenient to deal with Kepler orbits, our general definitions of the radial separation at crossing points and the angles between these points, and also our method of estimating phase differences, would be unchanged if we had chosen to consider orbits that are not closed (or trajectories that are not bounded).

We assert that the phase difference due to angular motion should be approximately $\Delta\Phi_2$. The arguments leading to this

assertion are as follows. A given final orbit would have associated with it two initial orbits whose relative orientation differs by the angle $\Delta\Phi_2-\Delta\Phi_1$. One of these initial orbits would have a crossing for inward motion, the other for outward motion. (These two initial orbits would be just one of many *pairs* of initial orbits—all with the same *relative* orientation—that would have to be taken into account in describing a transition from an initial state with angular dependence $Y_{L,L}$ to a final state with $Y_{L-1,L-1}$.) We consider motion directed initially inward, and starting on both initial orbits at the largest possible classically allowed radial separation. Even though these starting points are not in the region where quantum-mechanical motion is almost classical, we can assign to the two paths the initial phase difference

$$L(\Delta\Phi_2-\Delta\Phi_1),$$

which is simply the difference in phase between the relevant values of $Y_{L,L}$. The orbit with the larger phase is the one associated with a transition occurring as the $\bar{p}$ moves outward. The phases for the two separate paths leading to the same final orbit can be written as

$$\Phi_{\rm in}+(L-1)\Delta\Phi_2,$$

and

$$L(\Delta\Phi_2-\Delta\Phi_1)+\Phi_{\rm in}+L\Delta\Phi_1.$$

The first of these phases is associated with a transition occurring at the separation $R_c$ as the $\bar{p}$ moves inward on one of the two initial orbits, the second with a transition occurring at $R_c$ as it moves outward on the other. In writing down these two expressions, we have evaluated both phases at that point on the final orbit where the second transition occurs, and we have let $\Phi_{\rm in}$ denote the angular action that accumulates on either initial orbit as radial motion proceeds inward from its starting point to the first encounter with a point having the separation $R_c$. The phase that accumulates between the two successive encounters with the separation $R_c$ is $(L-1)\Delta\Phi_2$ on the first path and $L\Delta\Phi_1$ on the second. The difference between the phases for these two paths leading to the same final orbit is $\Delta\Phi_2$.

If phase differences due to angular motion—as estimated above for the special case of just two successive encounters with the avoided crossing, without even considering the width of the initial state—were the only phase differences that have to be taken into account, and if the motion were to proceed on true Kepler orbits, the separate contributions to the transition amplitude from not just two but many encounters of the $\bar{p}$ with the crossing would have just one of two phases. Half of them would have one phase, and half would have the other. (This would not generally be true for motion in a central field, but it would be true for closed orbits.) The difference between them would be $\Delta\Phi_2$. However, we believe there should be other, much smaller phase differences that would result in total incoherence. These other phase differences would be due to radial motion, and would take into account the finite width of the initial state. As outlined in Sec. III E 4, radial phase differences by themselves should result in incoherence if the width of the initial state were to be taken into account. To put the matter another way, phase differences due to different angular momenta on different paths should have no further effect on an estimated transition rate of $\bar{p}{\rm He}^+$ if the width of the initial state and radial phase differences are first taken into account. *However, we conjecture that the phase difference* $\Delta\Phi_2$ *might be important in the rather different type of Auger transition resulting in EAF. In such an instance there presumably would be only two encounters with an avoided crossing, and a large phase difference due to angular motion might be important.*

The preceding considerations are relevant to our Auger rates obtained with the modern BO approximation and probability currents. We note that $\Delta\Phi_2$ can be related, by means of an obvious generalization of the vector potential **A** defined in Eq. (4), to the change in phase of an *adiabatically varying* final electron wave function as the $\bar{p}$ moves on a final orbit from its first encounter with the crossing to its second. Our Auger calculations for $\bar{p}{\rm He}^+$ have thus far have not taken into account any adiabatic change in phase of this function, and for this reason it is necessary to redefine it. We also give it a more suitable normalization. We write

$$\psi_{2,\rm ad}(\mathbf{k},\mathbf{R},\mathbf{r})=\psi_2(\mathbf{k},\mathbf{r})e^{-i\Phi}/(2\pi)^{3/2},$$

where $\psi_2$ is defined in Eq. (11). The phase of $\psi_{2,\rm ad}$ depends on the azimuthal coordinate $\Phi$ of the position **R** of the $\bar{p}$. This function has the normalization

$$\int d^3k'\int d^3r\,\psi^*_{2,\rm ad}(\mathbf{k}',\mathbf{R},\mathbf{r})\,\psi_{2,\rm ad}(\mathbf{k},\mathbf{R},\mathbf{r})=1.$$

We now assume that the diagonal element $\mathbf{A}_{22}$ in Eq. (3) should be given, not by Eq. (4), which is really appropriate only for bound states, but instead by

$$\mathbf{A}_{22}=i\int d^3k'\int d^3r\,\psi^*_{2,\rm ad}(\mathbf{k}',\mathbf{R},\mathbf{r})\boldsymbol{\nabla}_{\boldsymbol{R}}\psi_{2,\rm ad}(\mathbf{k},\mathbf{R},\mathbf{r}).$$

It is obvious that $\Delta\Phi_2$ is given by

$$\Delta\Phi_2=\int_{\mathbf{R}_{c_1}}^{\mathbf{R}_{c_2}}\mathbf{A}_{22}(\mathbf{R})\cdot d\mathbf{R},$$

where the integration is over the path in the $x$-$y$ plane between the two successive crossing points $\mathbf{R}_{c_1}$ and $\mathbf{R}_{c_2}$ on a final orbit.

#### *4. Relative phases of reflected radial waves*

Within the framework of the procedures described in Secs. III A and III B, our numerical computations of outgoing, reflected, and multiply reflected radial waves were highly accurate. We were able to determine that there are small phase differences between waves traveling in the same direction on the same one-dimensional potential surface after having been reflected a different number of times. Partly because of the way our computer program had been written, but mostly because of the troublesome but transitory increases in the amplitude of the final state at separations much beyond the crossing, we found it convenient to examine only the wave function $v$ for motion on the diabatic surfaces, and evaluated only at the lower bound $R_{\rm lo}$ for classical motion on the upper adiabatic surface. (The functions $v$ and $w$ for mo-

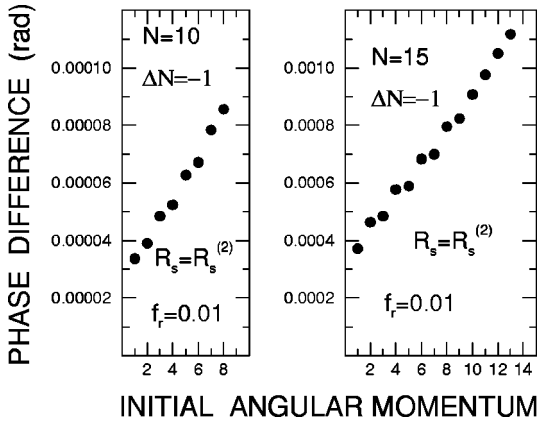


FIG. 12. The phase of the inward-traveling wave $v_1$ on the upper diabatic surface at $R_{lo}$ after two complete cycles relative to its phase after just one complete cycle. The phase scales for $N=10$ and 15 differ by a factor of 10.

tion on the diabatic and adiabatic surfaces are nearly the same at $R_{lo}$ if the initial and final orbitals are not circular or nearly circular.)

We first consider an example that is simple and instructive, though not directly relevant. Figure 12 shows the phase at $R_{lo}$ of the inward traveling wave $v_1$ on the upper diabatic surface after two complete cycles of radial motion relative to its phase at this point after just one complete cycle. Results were computed in each instance with $R_s=R_s^{(2)}$ and $f_r=0.01$. These phase differences are quite small, but they were found to vary linearly with $f_r$. These results, together with the transition probabilities shown in Fig. 5, indicate that in the realistic case $f_r=1.0$ a net change in phase exceeding $2\pi$ would be achieved after the completion of a number of half-cycles an order of magnitude smaller than the large number required before the transition becomes likely to have occurred. For example, in the case of the transition from the state with $N=15$ and $L=8$, these two numbers are $\sim 160$ and $\sim 1500$. In most other instances the relative difference is even larger. However, there is every reason to believe that if our calculations were to be extended to take into account many more reflections, the successive changes in the phase of $v_1$ at $R_{lo}$ would be nearly the same as those shown in Fig. 12. This presents a problem because we want to argue that the phases of many values of $v_1$, each obtained at the end of a *half*-cycle of radial motion, should not be almost uniformly spaced but should instead ultimately become a set of random numbers. We believe this could be accomplished by taking into account the finite width of the initial state.

If this width were to be taken into account, $v_1$ would be a superposition of many contributions, each corresponding to a different value of $E$. The finite time $\tau_A$ required for the transition implies that $E$ should have a range $\Delta E \sim \tau_A^{-1}$. This would introduce a range of phases associated with the radial motion. (There should also be a variation in phase associated with angular motion, but we have not attempted to estimate this.)

The range of phases is easily estimated for radial motion. The vibrational quantum number $n_v$ for the initial state should be given rather accurately by the WKB approximation. It can be regarded as a continuous function of $E$, and its derivative is given by

$$\frac{dn_v}{dE}=\frac{\tau_1}{2\pi},$$

where $\tau_1$ is the classically computed period of the initial state. This can be used to write

$$\Delta\phi=\pi\Delta n_v=\tau_1\Delta E/2\sim\tau_1/(2\tau_A),$$

where $\Delta\phi$ is the approximate range of the change in the radial action on the upper diabatic surface for a single half-cycle. Our approximate expression for $\Delta\phi$ in terms of $\tau_1$ and $\tau_A$ is numerically equal to the transition probability per half-cycle shown in Fig. 5. Though $\Delta\phi$ is small, its effect is cumulative: it should be multiplied by the number of half-cycles taken into account. This cumulative range of phase change in $v_1$ should ultimately exceed the phase difference for any two successive half-cycles, as estimated with $f_r=1.0$ for a fixed value of $E$. (In arriving at an estimate of the phase difference for any two successive half-cycles, we simply assume that, for a fixed value of $E$, this phase difference can be equated to the product of $f_r^{-1}$ and half the phase difference for the first two successive full cycles, as computed at $R_{lo}$ and shown in Fig. 12 for $f_r=0.01$.) The number of half-cycles required for this to occur is fairly small compared not only to the number required for the transition to become likely but also to the number required for the change in phase of $v_1$ to exceed $2\pi$ if $E$ is fixed. For example, in the case of the transition from the state with $n=15$ and $L=8$, this number is only $\sim 60$, as compared to $\sim 1500$ and $\sim 160$. In most other instances, the relative values of these three numbers are even more favorable to our argument. It therefore seems reasonable to conclude that the width of the initial state should ultimately cause the phases of most of a set of multiply reflected waves $v_1$, each evaluated after the completion of an integral number of half-cycles, to be effectively random.

The preceding discussion is only indirectly relevant to the question at hand. The relative phases of many *contributions* to $v_2$, each produced during a different half-cycle of motion, not the phases of many successive values of $v_1$, are what are directly relevant to our estimates of transition rates. Results of some calculations pertinent to this question are shown in Figs. 13 and 14. Figure 13 shows the absolute value of the phase of $v_2$ at $R_{lo}$ after two complete cycles relative to its phase after just one complete cycle. The sign of this relative phase is identified in every instance. As before, results were obtained with $R_s=R_s^{(2)}$ and $f_r=0.01$. Unfortunately, both the magnitude and the sign of this phase difference vary with $L$. However, the behavior of this phase difference seems to become less complicated as $f_r$ becomes larger. Figure 14 shows this phase difference—though on a different scale—if $f_r=0.001$, 0.01, or 0.1. It seems possible to extrapolate the results shown in Fig. 14, and obtain more or less reliable guessed values of the phase difference if $f_r=1.0$. We believe the results in Figs. 12–14 suggest that in the realistic case $f_r=1.0$ the range of the (presumably evenly spaced) phases of the *contributions* to $v_2$ after not too large a number of half-cycles, as computed for a fixed value of $E$, should be comparable to the net change in the phase of $v_1$. We further believe it would be reasonable to assume that these phases, like the phases of values of $v_1$ obtained after integral num-

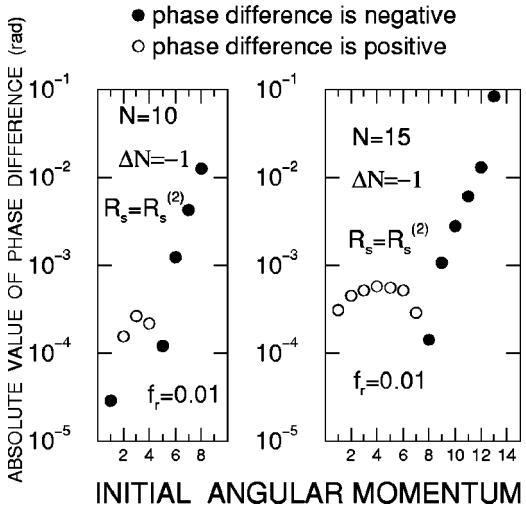


FIG. 13. The absolute value of the phase of the inward-traveling wave $v_2$ on the lower diabatic surface at $R_{lo}$ after two complete cycles relative to its phase at this point after just one complete cycle. The sign of this relative phase is identified in every instance.

bers of half-cycles, would become effectively random after not too large a number of reflections if the width of the initial state were to be taken into account, thereby causing the contributions to the transition amplitude from separate half-cycles of $\bar{p}$ motion to be incoherent.

## IV. DISCUSSION

### A. Auger rates for metastable $\bar{p}He^+$

We have used the modern BO approximation to estimate Auger rates for some unrealistically low-lying states of $\bar{p}He^+$. The question arises as to whether it could also be used to calculate rates for the metastable states, which are much more highly excited. We believe that this could be done, at least in principle. But as explained below, we also believe that it should be done with the golden rule, not probability currents. Such a calculation would, of course, require traditional BO wave functions and energies. These have already been calculated precisely for the metastable states [25,26]; and it seems possible to obtain, if necessary, precise electronic BO functions for the final states [35]. Nonetheless, a golden rule calculation for a metastable state would appear to be difficult—perhaps even ill advised if the two-state approximation used in the present paper were to be retained—and we briefly mention some of the problems, and also some of the advantages.

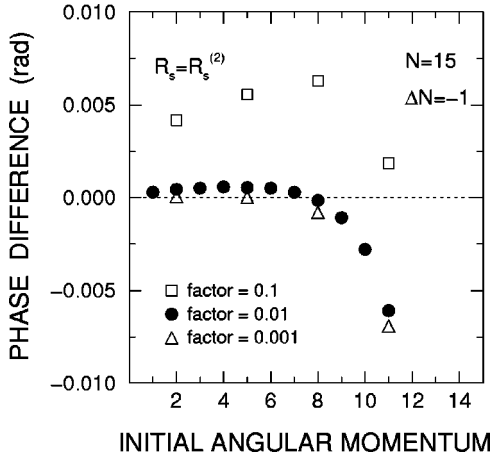


FIG. 14. The phase of the inward-traveling wave $v_2$ on the lower diabatic surface at $R_{lo}$ after two complete cycles relative to its phase at this point after just one complete cycle, as computed with different values of the multiplicative factor $f_r$.

One problem is the possible importance of second-order effects. The states in question are metastable, not because the perturbing interaction is in general especially small, but because the final electron—which has a low energy (substantially less than 1 a.u.) and a high angular momentum ($\Delta L \geqslant 4$)—has very little overlap with the initial electron. Though taking into account only first-order transitions should lead to estimates that are at least approximately correct, the very low rates seem by themselves to be no guarantee that these estimates would be highly accurate. The first rate estimates for metastable $\bar{p}He^+$ were made using some very simple variational wave functions and the golden rule, with the initial electron wave function having no angular dependence on the position of the slowly moving $\bar{p}$, and with the perturbation being the electrostatic interaction of multipole order $\Delta L$ between the $\bar{p}$ and the electron [36]. Subsequently, rates have been computed using vastly more accurate variational wave functions [37–43]. But to our knowledge there has, within the framework of the modern BO approximation, been no reliable determination that virtual transitions of lower multipole order to and from intermediate states introduce no significant correction.

Metastable $\bar{p}$ orbitals are circular or nearly circular. As illustrated in Fig. 8, rate estimates obtained with probability currents for relatively low-lying circular orbitals are not very accurate. If only for this reason, we believe that an Auger calculation for metastable states using BO wave functions should employ the golden rule, not probability currents. In at least one respect, the modern BO approximation would appear to be especially suited for a golden rule calculation: it distinguishes that part of the $\bar{p}$-electron interaction which is responsible for the transition from that part which merely distorts the initial and final wave functions. It would be analogous to the distorted-wave Born approximation. The Hamiltonian for the $\bar{p}$ would be written in the form given in Eqs. (5) and (6), but with $M$ now being the reduced mass of the $\bar{p}$ and the He nucleus, and with $V(R)$ now being

$$V(R)=\begin{pmatrix} -\frac{2}{R}+\epsilon_1(R) & 0 \\ 0 & -\frac{2}{R}+\epsilon_2 \end{pmatrix},$$

where $\epsilon_1$—which now depends on $R$—is the energy of the adiabatically varying initial electronic state, as obtained in a traditional BO calculation. As with the transitions considered in the present paper, the energy $\epsilon_2$ of the final electronic state should be constant and equal to $\frac{1}{2}k^2$ because this state is in the continuum. The unperturbed wave functions would simply be $\bar{p}$ functions computed with the traditional BO approximation. The perturbing interaction $H'$ would be given

by Eq. (6b). A second advantage of a golden rule calculation using the modern BO approximation is that center-of-mass corrections of the type discussed in Ref. [16] are included implicitly in the expression for $H'$ if the electronic BO wave functions are computed precisely.

The interaction $H'$ and its matrix elements would probably not be easy to calculate accurately for highly excited states, even if only first-order transitions have to be taken into account. Unlike the estimates presented in the present paper for relatively low-lying states, the calculations could not be carried only to lowest nonvanishing order in $R$, which means that the determination of $\mathbf{A}$ would be more difficult, largely because $\boldsymbol{\nabla}_{\boldsymbol{R}}\psi_1(\mathbf{R},\mathbf{r})$ would no longer be independent of $R$, as it is in the calculations outlined in Sec. II C. Moreover, because of the large change in the $\bar{p}$ angular momentum, it would be necessary to determine accurately that very small part of $H'$ which transforms under rotations about the $z$ axis as $\exp(-i\Delta L\phi)$.

### B. Exotic atom formation

We now present a summary and a slightly more detailed discussion of our conjecture about the role in EAF of phase differences due to angular motion. This conjecture, which was made in Sec. III E 3, is based in part on (i) our conclusion in Sec. III D 2 that an Auger transition from a low-lying level of $\bar{p}\mathrm{He}^+$ can be thought of as occurring at rather well-defined points, in accord with the FCP, and (ii) our estimates of a large, $L$-dependent angular separation $\Delta\Phi_2$ between such points, as shown in Fig. 11(b) for Kepler orbits. However, we must acknowledge that our estimates of Auger rates using the modern BO approximation and probability currents do not really demand that phase differences due to angular motion be important in $\bar{p}\mathrm{He}^+$. As explained in Sec. III E 4, our estimates can very likely be made to agree fairly well with the golden rule by taking into account only phase differences associated with radial motion, together with the width of the initial state. But our calculations are entirely consistent with the presence of phase differences due to angular motion, and we believe their presence is in fact strongly suggested. These results—together with the regularities in x-ray yields reported in Refs. [4–9], which we suspect are due to interference—have prompted our conjecture about EAF. Specifically, we have conjectured that the x-ray data can largely be accounted for by a difference in angular action along different paths leading to the same final state. Furthermore, we have suggested that the phase difference due to this difference in angular action could be estimated by employing classical trajectories for the initial states and a classical orbit for the final state, much as we have done with Kepler orbits for $\bar{p}\mathrm{He}^+$ in Secs. III E 2 and III E 3.

Our conjecture is contingent upon EAF being a nonresonant reaction. We imagine EAF as occurring during just one, simple, almost classical collision of the stopping hadron or muon with the capturing atom. Even though it is a reaction, not a decay, there are clear similarities to the sort of Auger transition considered in the present paper. As noted in Sec. I, it has long been widely believed that EAF is an almost adiabatic process; so it should be possible to describe it within the framework of the modern BO approximation. As we have concluded for Auger transitions in $\bar{p}\mathrm{He}^+$, the FCP should be relevant: one should be able to think of EAF as occurring during radially rather well-defined encounters with an avoided crossing. Presumably, there would be just two encounters, not the large numbers considered in the present paper. Therefore, one should be able to think of the transition amplitude as a coherent sum of two contributions, one produced as the stopping particle first moves inward toward the nucleus of the capturing atom, the other as it then attempts to move away. There might be a significant difference in phase between these two contributions. In general, this difference could be due to both radial and angular motion. In the present paper we have found, for the special case of successive encounters with an avoided crossing in low-lying levels of $\bar{p}\mathrm{He}^+$, that there is only a small difference in phase due to radial motion, but we have found there is a large, $L$-dependent difference $\Delta\Phi_2$ due to angular motion.

The present calculations give no clear indication as to how the $L$ dependence of $\Delta\Phi_2$ would vary with atomic number in the case of EAF. But it does seem reasonable to expect that there could be a significant dependence. This phase difference should be determined by the size and shape of the adiabatically varying effective radial potentials experienced by the stopping particle in both the initial and final states, and also by the energy this particle loses when it is captured. The detailed behavior of these potentials, as well as the energy loss, should depend on atomic number. (The possible relevance of atomic size to EAF was noted many years ago by Condo [44].) The very fact that $\Delta\Phi_2$ could depend in more than one way on atomic number is itself encouraging, because x-ray yields accompanying EAF, unlike most shell-dependent properties of atoms, appear to vary more or less smoothly in the vicinity of closed shells [4–6]. This suggests that more than one atomic property must be taken into account. These questions are being investigated.

### ACKNOWLEDGMENTS

J. Oldendick gave valuable assistance in the preparation of some of the figures. Some of the work reported here was supported in part by NSF Grant No. PHY-8706863.

[1] J. Franck, Trans. Faraday Soc. **21**, 536 (1925).
[2] E. U. Condon, Phys. Rev. **32**, 858 (1928).
[3] See, for example, W. H. Miller, in *Advances in Chemical Physics*, edited by I. Prigogine and S. A. Rice (Wiley, New York, 1974), Vol. 25, p. 69.
[4] C. E. Wiegand and G. L. Godfrey, Phys. Rev. A **9**, 2282 (1974).
[5] D. Quitmann *et al.*, Nucl. Phys. **51**, 609 (1964).
[6] V. G. Zinov, A. D. Konin, and A. I. Mukhin, Yad. Fiz. **2**, 859 (1965) [Sov. J. Nucl. Phys. **2**, 613 (1966)].

[7] See, for example, T. von Egidy *et al.*, Phys. Rev. A **23**, 427 (1981).
[8] See, for example, C. J. Orth *et al.*, Phys. Rev. A **25**, 876 (1982).
[9] See, for example, T. von Egidy and F. J. Hartmann, Phys. Rev. A **26**, 2355 (1982).
[10] G. Backenstoss, Contemp. Phys. **30**, 433 (1989).
[11] T. Yamazaki, Nucl. Phys. A **585**, 215c (1995).
[12] See, for example, the bibliography compiled by D. Horváth and R. M. Lambrecht, *Exotic Atoms* (Elsevier, Amsterdam, 1984).
[13] G. Ya. Korenman and S. N. Yudin, Pis'ma Zh. Eksp. Teor. Fiz. **58**, 10 (1993) [JETP Lett. **58**, 9 (1993)]; Few-Body Syst., Suppl. **7**, 204 (1994).
[14] W. A. Beck, L. Wilets, and M. A. Alberg, Phys. Rev. A **48**, 2779 (1993).
[15] B. L. Druzhinin, A. E. Kudryavtsev, and V. E. Markushin, Pis'ma Zh. Eksp. Teor. Fiz. **58**, 236 (1993) [JETP Lett. **58**, 241 (1993)].
[16] Z. Fried and A. D. Martin, Nuovo Cimento **29**, 574 (1963).
[17] See, for example, B. Ketzer *et al.*, Phys. Rev. Lett. **78**, 1671 (1997), and references therein.
[18] G. R. Burbidge and A. H. de Borde, Phys. Rev. **89**, 189 (1953).
[19] J. E. Russell, Hyperfine Interact. **103**, 359 (1996).
[20] P. Pechukas, Phys. Rev. **181**, 166 (1969).
[21] W. H. Miller and T. F. George, J. Chem. Phys. **56**, 5637 (1972).
[22] B. Zygelman, Phys. Lett. A **125**, 476 (1987).
[23] J. Moody, A. Shapere, and F. Wilczek, in *Geometric Phases in Physics*, edited by A. Shapere and F. Wilczek, Advanced Series in Mathematical Physics Vol. 5 (World Scientific, Singapore, 1989), p. 160.
[24] I. Shimamura, Phys. Rev. A **46**, 3776 (1992).
[25] P. T. Greenland and R. Thürwächter, Hyperfine Interact. **76**, 355 (1993).
[26] F. Wilczek and A. Zee, Phys. Rev. Lett. **52**, 2111 (1984).
[27] M. V. Berry, Proc. R. Soc. London, Ser. A **392**, 45 (1984).
[28] T. G. Heil and A. Dalgarno, J. Phys. B **12**, L557 (1979).
[29] See, for example, E. Merzbacher, *Quantum Mechanics*, 2nd ed. (Wiley, New York, 1970), p. 475.
[30] See, for example, L. D. Landau and E. M. Lifshitz, *Quantum Mechanics, Non-Relativistic Theory*, 2nd ed. (Pergamon, Oxford, 1965), p. 326.
[31] D. R. Bates, Proc. R. Soc. London, Ser. A **257**, 22 (1960).
[32] W. R. Thorson, J. B. Delos, and S. A. Boorstein, Phys. Rev. A **4**, 1052 (1971).
[33] W. H. Miller, in *Advances in Chemical Physics*, edited by K. P. Lawley (Wiley, New York, 1975), Vol. 30, p. 84.
[34] See, for example, A. Messiah, *Quantum Mechanics* (North-Holland, Amsterdam, 1965), Vol. I, pp. 222–228; see also K. Gottfried, *Quantum Mechanics* (Benjamin, Reading, 1966), Vol. I, pp. 70–74.
[35] P. T. Greenland, Theor. Chim. Acta **38**, 185 (1975); see also P. T. Greenland and W. Greiner, *ibid.* **42**, 273 (1976).
[36] J. E. Russell, Phys. Rev. A **1**, 742 (1970).
[37] K. Ohtsuki (unpublished).
[38] N. Morita, K. Ohtsuki, and T. Yamazaki, Nucl. Instrum. Methods Phys. Res. A **330**, 439 (1993).
[39] O. I. Kartavtsev, Yad. Fiz. **59**, 1541 (1996) [Phys. At. Nucl. **59**, 1483 (1996)].
[40] O. I. Kartavtsev, S. I. Fedotov, and D. E. Monakhov, Hyperfine Interact. **109**, 125 (1997).
[41] V. I. Korobov, Nucl. Phys. B (Proc. Suppl.) **56A**, 89 (1997).
[42] V. I. Korobov and I. Shimamura, Phys. Rev. A **56**, 4587 (1997).
[43] J. Révai and A. T. Kruppa, Phys. Rev. A **57**, 174 (1998).
[44] G. T. Condo, Phys. Rev. Lett. **33**, 126 (1974).